Univerzita Karlova v Praze

1. lékařská fakulta

Studijní program: Biomedicína

Studijní obor: Fyziologie a patofyziologie člověka

MUDr. Marek Šramko

Využití magnetické rezonance srdce pro posouzení patofyziologie dilatační kardiomyopatie.

Use of cardiovascular magnetic resonance for evaluation of pathophysiollogy in dilated cardiomyopathy.

Disertační práce

Školitel: MUDr. Miloš Kubánek, Ph.D.

Praha, 2014

Prohlášení

Prohlašuji, že jsem závěrečnou práci zpracoval samostatně a že jsem řádně uvedl a citoval všechny použité prameny a literaturu. Současně prohlašuji, že práce nebyla využita k získání jiného nebo stejného titulu. Souhlasím s trvalým uložením elektronické verze své práce v databázi systému meziuniverzitního projektu Theses.cz za účelem soustavné kontroly podobnosti kvalifikačních prací.

V Praze, 10.9.2014

Marek Šramko

Indentifikační záznam (Referencing)

Šramko, Marek. *Využití magnetické rezonance srdce pro posouzení patofyziologie dilatační kardiomyopatie. [Use of cardiovascular magnetic resonance for evaluation of pathophysiollogy in dilated cardiomyopathy.]* Praha, 2014, 72s, 2 příl. Disertační práce (Ph.D.). Univerzita Karlova v Praze, 1. lékařská fakulta, Fyziologický ústav. Školitel Kubánek, Miloš.

Acknowledgement

I would like to express my deepest gratitude to my tutor, Dr. Miloš Kubánek, for his patient guidance and assistance throughout the research.
My sincere appreciation goes also to my coworkers, Dr. Malušková, Dr. Kautznerová, Ing. Tintěra and Dr. Weichet, for excellent collaboration and valuable advices and to Professor Kautzner for his academic support.
Above all, my deepest gratitude belongs to my wife, Riina, for all the support during my research.

Contents

List of Tables

List of Figures

List of Abbreviations

ACEI = angiotensin-converting-enzyme inhibitor

ARB = angiotensin receptor blocker

BMI = body mass index

BNP = B-type natriuretic peptide

BP = blood pressure

CMR = cardiovascular magnetic resonance

DCM = dilated cardiomyopathy

ECG = electrocardiography

GFR = glomerular filtration rate

EDD = enddiastolic dimension

EDV = enddiastolic volume

EGE = early gadolinium enhancement

EMB = endomyocardial biopsy

Hs-TnT = high-sensitivity troponin T

LA = left atrium / left atrial

LGE = late gadolinium enhancement

LV = left ventricle / left ventricular

LVRR = left ventricular reverse remodelling

NYHA = New York Heart Association (functional class)

RV = right ventricle / right ventricular

TAPSE = tricuspid annular plane systolic excursion

Souhrn (abstract in Czech)

Dilatační kardiomyopatie (dilated cardiomyopathy, DCM) je druhou nejčastější příčinou srdečního selhání. Patofyziologie DCM není zcela objasněna. Jedním z důvodů jsou limitace současných klinických metod pro výzkum tohoto onemocnění. Cílem této práce bylo posudit schopnost magentické rezonance srdce (cardiovascular magentic resonance, CMR), s využitím moderních zobrazovacích technik, pro in vivo vyšetření některých klíčových patofyziolgických mechanizmů, které mají s DCM přímou souvislost. Dalším cílem práce bylo pousoudit, zda patologické nálezy na CMR umožní předpovědět klinicky relevantní zlepšení morfologických a funkčních parametrů levé komory srdeční – reverzní remodelaci (left ventricular reverse remodelling, LVRR).

U 44 pacientů s nově manifestovanou DCM (délka trvání <6 měsíců) byla provedena CMR, endomyokardiální biopsie, zátěžové vyšetření a vyšetření srdečních biomarkerů. CMR byla zopakována po 12 měsících klinického sledování.

U 34 % pacientů byly pomocí biopsie zjištěny zánětlivé změny myokardu. LVRR byla po 12 měsících pozorována u 45 % pacientů. Přítomnost pozdního sycení gadolinia (late gadolinium enhancement, LGE) v levé komoře byla senzitivním ale málo specifickým znakem zánětu myokardu, protože přítomnost LGE byla taktéž projevem hemodynamického zatížení při srdečním selhání. Rozsah LGE byl nezávislým prediktorem LVRR a taktéž prediktorem závažných klinických událostí. Přítomnost perikardiálního výpotku a zvýšené časné sycení gadolina byly specifickými ale málo častými známkami zánětu myokardu. Vyšetření edému myokardu pomocí T2-vážených sekvencí nebylo přínosné pro detekci zánětu myokardu, avšak ukázalo se užitečné pro predikci LVRR.

Lze tedy uzavřít, že CMR se jeví jako suboptimální metoda pro detekci zánětu myokardu u pacientů s nově manifestovanou DCM. Nicméně, u těchto pacientů může CMR odhalit poškození myokardu v souvislosti s hemodynamickým zatížením a navíc umožňuje spolehlivě predikovat LVRR.

Klíčová slova: patofyziologie, kardiomyopatie, zánět myokardu, reverzní remodelace, magnetická rezonance

Abstract

Dilated cardiomyopathy (DCM) is the second leading cause of heart failure. The pathophysiology in DCM is still poorly understood, partly because of currently limited research tools. We investigated whether cardiovascular magnetic resonance (CMR), using novel imaging techniques, could be used for in vivo assessment of some key pathophysiological mechanisms related to DCM. In addition, we evaluated whether the pathological findings on CMR would predict clinically relevant functional and morphological improvement of the left ventricular (LV) function – the left ventricular reverse remodeling (LVRR).

CMR together with endomyocardial biopsy, echocardiography, cardiopulmonary exercise testing and a thorough assessment of cardiac biomarkers was performed in 44 patients with new-onset DCM (<6 months of duration). The imaging was repeated after 12 months of clinical follow-up.

Endomyocardial biopsy revealed myocardial inflammation in 34 % of the patients. LVRR at 12 months occurred in 45 % of the patients. Presence of late gadolinium enhancement (LGE) in the left ventricle was a sensitive but unspecific sign of myocardial inflammation because it was also a feature of hemodynamic stress related to the heart failure. The baseline extent of LGE was an independent predictor of future LVRR and also a predictor of adverse clinical events. Pericardial effusion and increased early gadolinium enhancement were specific but uncommon signs of myocardial inflammation. Assessment of myocardial edema by T2-weighted imaging did not add value to detection of myocardial inflammation but it was valuable for predicting of LVRR.

In conclusion, CMR seems a suboptimal method for detection of myocardial inflammation in new-onset DCM. However, in these patients CMR may reveal myocardial injury related to hemodynamic stress and it may predict future LVRR.

Key words: pathophysiology, cardiomyopathy, myocardial inflammation, reverse remodeling, cardiovascular magnetic resonance

1 Introduction

1.1 Scope of the problem

Dilated cardiomyopathy (DCM) is a heart disease in which the left ventricle (LV) becomes dilated, thin-walled and dysfunctional. The reduction of the LV stroke volume typically manifests with heart failure. In fact, DCM is after the coronary artery disease the second leading cause of chronic heart failure with a prevalence of 40-50/100,000 in the adult population (Mosterd & Hoes 2007).

Although the LV function may improve or even fully recover in some individuals, the overall prognosis of the patients with DCM remains poor (Merlo et al. 2014). A heart transplantation or implantation of a ventricular assist device are often the only therapeutic options (Baldasseroni et al. 2002).

Etiology of DCM is multifactorial and often difficult to establish in clinical practice, even with contemporary diagnostic methods. Consequently, pathophysiology of the disease is still poorly understood (Elliott et al. 2008). However, a better recognition of the underlying pathophysiology is a critical prerequisite for development of new more specific therapeutic approaches and also for individualization of the management of DCM patients (Frustaci et al. 2009).

The lack of understanding of the pathophysiology in DCM may be largely explained by the limitations of the currently available methods for investigating important pathological processes in vivo (in particular myocardial inflammation and fibrosis). This motivates the researchers to search for more reliable diagnostic tools. Ideally, such method would not only provide insights in the pathophysiology of DCM but it could be applied also to the daily clinical practice. In this regard, cardiovascular magnetic resonance (CMR) using novel imaging techniques holds promises (Friedrich et al. 2009), but its role in DCM remains to be clarified.

1.2 Etiology of dilated cardiomyopathy

As indicated above, DCM is etiologically a heterogeneous disease, even though it presents with an invariable morphological phenotype. The diagnosis of DCM can be established only after excluding coronary artery disease, severe arterial hypertension, primary valve disease or a congenital heart condition as possible causes of the ventricular dysfunction (Richardson et al. 1996, Elliott et al. 2008). Table 1 provides an overview of the etiological factors which have been related to the disease.

Table 1: Etiological factors associated with DCM

Familial forms of DCM	Acquired forms of DCM
Familial, unknown gene	Myocarditis
	– Infectious (viruses, bacterias, protozoa)
Mutation of sarcomeric proteins	– Toxic
– β-myosin heavy chain	– Autoimmune
– Cardiac myosin binding protein	
– Troponin I	Kawasaki disease
– Troponin T	
– α-tropomyosin	Eozinophilic (Churg-Strauss) syndrome
– Essential myosin light chain	
– Actin	Cytotoxic
– α myosin heavy chain	– Alcohol
– Titin	– Amphetamines, cocaine
– Troponin C	– Doxorubicin
	– Bleomycin
Genes for Z-band proeins	– 5-Fluorouracyl
– Muscle LIM protein	
– TCAP	Nutritional diseases
	– Selenium
Cytoskeletal genes	– Thiamine
– Dystrophin	– Carnitine
– Desmin	– Hypocalcaemia
– Metavinculin	– Hypophosphataemia
– Sarcoglycan complex	
– CRYAB	Metabolic diseases
– Epicardin	
	Endocrine diseases
Genes for nuclear membrane proteins	
– Lamin A/C	Sarcoidosis
– Emerin	
	Tachycardic cardiomyopathy
Intercalated disc protein mutations	
– Pakoglobin	Pregnancy
– Desmoplakin	
– Plakofilin 2	
– Desmoglein 2	
– Desmocolin 2	
Mitochondrial cytopathy	

Adopted from Elliott et al. (2008)

A systematic cardiologic screening may reveal DCM in a first-degree relative in 30–35 % of the DCM patients (Hershberger et al. 2009). But a particular genetic cause cannot be identified in up to two thirds of the familial cases of DCM, despite ever-increasing availability of the next generation sequencing methods. The most common genetic defects include truncating mutations of titin (25 % of familial and 18 % of sporadic cases) and mutations of lamin A/C (4–8 %), followed by various rare mutations of genes coding proteins of sarcomere, Z-disc, cytoskeleton, nuclear envelope, mitochondria, sarcoplasmic reticulum, metabolic pathways and transcription factors (Lopes & Elliott 2013).

Acquired forms of DCM have been associated with a number of toxic agents, metabolic and endocrine disease. Above all, the far most common etiology of an acquired DCM is myocarditis, which can be found in about one third of the DCM patients (Kawai 1999). Impairment of the ventricular function may result either from direct myocyte injury by an infectious agent (usually by a virus), or the otherwise benign agent may merely trigger a pathological autoimmune response (Kawai 1999, Caforio & Iliceto 2008). If the DCM develops in the presence of myocarditis the disease is called inflammatory DCM. Often no specific cause can be determined – in that case the DCM is called idiopathic (Richardson et al. 1996).

Disclosing the etiology of DCM in an affected individual may be clinically important. It may provide an opportunity for applying an etiology-specific therapy on top of the standard management of heart failure. For example, an early implantation of a cardioverter-defibrillator for primary prevention of sudden cardiac death is recommended in DCM patients with pathogenic mutation of lamin A/C, because they have a high risk of malignant arrhythmias (Pasotti et al. 2008). Identification of familial forms of DCM enables to initiate an appropriate treatment in affected relatives. Selected patients with myocarditis can be treated with antiviral agents, antibiotics (Lyme carditis) or immunosuppressive treatment. Corticosteroids may be effective for treatment of cardiac sarcoidosis. At last, specific treatment exists also in DCM that is associated with some rare metabolic diseases (hemochromatosis) and endocrine disease (hypothyroidism).

1.3 DCM and left ventricular reverse remodeling

DCM involves changes in cardiac structure, myocardial composition and multiple functional alterations at the cellular level, all of them contributing to the progressive LV dilatation and dysfunction (Koitabashi & Kass 2012). The process of stopping and reverting these changes (either naturally or with treatment) is commonly known as left ventricular reverse remodeling (LVRR). More strictly, LVRR refers to an increase of the LV ejection fraction which is accompanied by reduction

of the LV enddiastolic volume (Koitabashi & Kass 2012). From a clinical perspective, occurrence of LVRR is important because it forecasts a favorable long-term prognosis (Pasotti et al. 2008). Thus, achieving the LVRR by any effective means in an affected individual belongs to the main objectives in the management of DCM.

In contrast to the clinical evidence confirming the central role of LVRR in a successful treatment of DCM, far less is known about the underlying pathophysiological mechanisms of this phenomenon. The LVRR in DCM has been explained either by the resolution of the underlying pathological process—such as healing of myocarditis—or by the beneficial effect of the pharmacotherapy. However, individual contribution of each of these mechanism is unknown.

For research of LVRR, patients with new-onset DCM (<6 months of duration) seem to be a particularly interesting subpopulation of DCM. LVRR occurs in up to a half of these patients, though a full LV recovery is uncommon (Dec 2014, Bello et al. 2011). In contrast, in chronic DCM (>6 months of duration) LVRR is less frequent and the LV dysfunction is often permanent. Moreover, the initial insult may not be present at a later phase of the disease (Friedrich et al. 1998). For the reasons above this work focused primary on the subgroup of the new-onset DCM.

1.4 Current „golden standard“ method for assessment of myocardial tissue pathology in clinical practice

Endomyocardial biopsy (EMB) is currently regarded the „golden standard” method for in vivo assessment of myocardial tissue characteristics in cardiomyopathies. The bioptome is usually introduced into the right ventricle through a transjugular or transfemoral approach. Myocardial samples (5-8 pieces, each of them about $1mm^3$ large) are harvested from the right side of the interventricular septum. Histopathological and immunohistochemical assessment of the specimens enables to detect a number of tissue processes, including the presence and activity of inflammatory cells, extent of myocyte necrosis and interstitial replacement fibrosis (Loud & Anversa 1984, Frustaci et al. 2009). In addition, the EMB can reveal a specific cause of the heart failure, such as sarcoidosis, or a storage disease (hemochromatosis, amyloidosis, glycogenosis or Fabry disease).

However, EMB has several noteworthy limitations. First, due to its invasive character the procedure carries a non-negligible risk of serious complications. These include pneumothorax, cardiac tamponade and life-threatening arrhythmias (Cooper et al. 2007). Second, EMB is limited by sampling bias – focal pathologi-

cal processes may be missed if the specimens were harvested from a distant site. The sampling bias can be partially overcomed by obtaining additional samples, by obtaining samples from inside of the LV cavity or by targeting the biopsy to a site which appeared pathological on a preceding imaging modality (Hauck et al. 1989, Chow et al. 1989, Shirani et al. 1993). However, such alternative approaches increase the risk of procedural complications. At last, EMB is limited by a substantial inter-indiviudal variablity in the interpretation of the specimens (Shanes et al. 1987). Immunohistochemistry provides a more detailed information about the tissue pathology but its use is restricted by availability, high cost and lack of standardization of diagnostic criteria.

1.5 The potential of CMR

CMR is a versatile and widely-available imaging modality, which does not expose the patient to any radiation. Besides detailed assessment of cardiac morphology and function, the imaging enables to directly visualize some key pathological myocardial tissue processes that have a verified histological and pathophysiological correlate. These include edema, hyperemia, capillary leakage, myocardial necrosis and interstitial fibrosis (Friedrich et al. 2009).

Since its introduction into clinical practice CMR has been used mainly for evaluation of myocardial viability in the patients with ischemic heart disease. However, recent advances in the CMR technology and imaging techniques allowed to extend this modality also to other, more refined applications. The following paragraphs describe in details the main diagnostic targets for CMR and their application in in the context of DCM.

1.5.1 Ventricular morphology and function

Cardiac morphology and function is usually assessed by so-called "kinetic" sequences. The main advantage of these scans are an excellent image contrast and a high temporal and spatial resolution. These assets enable an accurate and highly reproducible quantification of morphological and functional parameters of the left and right ventricle. The high reproducibility of the volumetric measurement is particularly important for serial evaluation of changes in the LV volume during the course of the disease.

Although in DCM the LV dilatation and systolic dysfunction is not specific for a particular etiology, transient LV wall abnormalities along with a transient increase in LV mass can serve to retrospectively confirm resolving myocardial inflammation (Hiramitsu et al. 2001, Zagrosek et al. 2009).

At last, thanks to the high pixel resolution of the images, CMR often reveals a specific morphological phenotype, which would be otherwise missed by another imaging modality. As an example, a finding of excessive trabeculation of the LV endocardium is specific for non-compaction cardiomyopathy (Virtova et al. 2013).

1.5.2 Pericardial effusion

Pericardial effusion may occur in a number of systemic conditions, including cancer, renal failure and autoimmune diseases, though in otherwise healthy individuals the far most common cause of the effusion is a viral pericarditis or perimyocarditis (Karjalainen & Heikkila 1986, Ammann et al. 1986). CMR can visualize the effusion with a high resolution, thus allowing an accurate quantification of its volume by planimetry (Ong et al. 2011). Small accumulation of pericardial fluid that is not circumferential is usually not pathologic. On the other hand, circumferential effusion (>50ml) that contains non-fluid components (such as fibrinous deposits or thrombi) is always regarded pathologic (Bogaert & Francone 2009).

1.5.3 Myocardial edema

Edema is an integral part of cellular injury. A mild insult causes only functional alterations in the permeability of the cellular membrane. This typically leads to influx of sodium ions, which is followed by an increase in the intracellular water content - intracellular edema. A more severe insult causes impairment of the membrane integrity, which leads to leakage of large molecules and efflux of net water to the extracellular space - extracellular edema. Loss of the large molecules further aggravates the cellular functions and eventually leads to cellular necrosis.

CMR can visualize the edema by detecting water-bound protons by T2-weighted imaging (Friedrich et al. 2009). On the T2-weighted images the regions with a greater water content appear brighter than a surrounding normal tissue. However, in some patients the edema may be distributed diffusely in the LV myocardium, thus limiting a comparison of regional differences in the signal intensities within the myocardium. Therefore the signal intensity of the myocardium is usually compared with the intensity of a healthy skeletal muscle within the image view. A ratio of the two respective signal intensities (also called "edema ratio") of >1.9 indicates myocardial edema (Friedrich et al. 2009).

The ability of CMR to detect myocardial edema has been validated in the setting of acute myocardial infraction and in histologically-verified acute myocarditis (Friedrich et al. 2009). However, the role of the T2-weighted imaging in the patients with DCM has not yet been established. In fact, these patients are likely

to have less pronounced edema than those with acute myocardial infarction or clinically overt acute myocarditis (Gutberlet et al. 2008).

1.5.4 Hyperemia and capillary leakage

Local vasodilatation along with increased permeability of capillaries for water and large molecules belong to key pathophysiological processes in tissue inflammation. The increased intravascular and interstitial space can be visualized by T1-weighted imaging with application of gadolinium contrast. After intravenous injection the water-soluble contrast agent rapidly distributes to interstitial space. The increased interstitial space accumulates a greater amount of the contrast than a healthy tissue. Consequently, the affected myocardial regions appears brighter on the T1-weighted imaging than healthy myocardium. The dilated capillaries also contain more of the contrast but these changes are negligible compared to the volume changes in interstitium. Similarly as in the assessment of edema, the signal intensity of the myocardial tissue must be related to a healthy skeletal muscle within the same image. An index of the relative increase in the overall LV signal intensity is known as early gadolinium enhancement ratio (EGE).

The technique of EGE was validated in induced hyperemia (Miller et al. 1989). Clinically, it has been used for detection of inflammation of skeletal and also myocardial muscle (Paajanen et al. 1987, Friedrich et al. 1998, Abdel-Aty et al. 2005).

1.5.5 Myocardial necrosis and replacement fibrosis

Ongoing myocardial necrosis and subsequent fibrotic scarring can be assessed by the technique of late gadolinium enhancement (LGE). Technical implementation of the LGE sequence is similar to the EGE, only that the acquisition of the LGE images begins 10–15 minutes after administration of the contrast Kim et al. (2000).

In a healthy myocardium this time is sufficient for most of the contrast to diffuse from the interstitial space back to blood, from where it is removed by renal excretion. However, if the tissue contains excessive interstitial fibrosis (scar) the large chelates of gadolinium are entrapped in the fibrotic matrix. Although the contrast is eventually washed-out also from the fibrotic myocardium it may take up to one hour. Therefore the fibrotic regions remain brighter (enhanced) for much longer time than a healthy myocardium (see Figure 1).

Under normal conditions the gadolinium chelates cannot enter inside the myocyte. However, if the cellular membrane is being disrupted (for example, by ischemia or inflammation) the contrast diffuses also in the intracellular space.

Consequently, the necrotic tissue contains relatively greater amount of the contrast and it appears brighter than a surrounding healthy myocardium.

LGE is currently considered a golden standard for in vivo detection of myocardial necrosis (whether ongoing or healed with scar); the technique has been validated by numerous studies in an animal model and in human. It must be underlined, however, that LGE cannot discriminate active ongoing necrosis from a healed fibrotic scar. On the other hand, the pattern and regional distribution of the LGE can often hint the underlying etiology. In particular, while in the coronary artery disease the LGE follows an ischemic wave-front from the endocardium towards the epicardium, the LGE of non-ischemic etiology typically presents as blurry stripes or patches localized anywhere in the LV and it rarely occurs in the subendocardium (Mahrholdt et al. 2005).

Importantly, the extent of LGE in the LV can be accurately quantified by means of manual planimetry or by a thresholding technique. Exact quantification of the LGE is particularly important for serial CMR studies.

Figure 1: Pathophysiological principle of LGE.

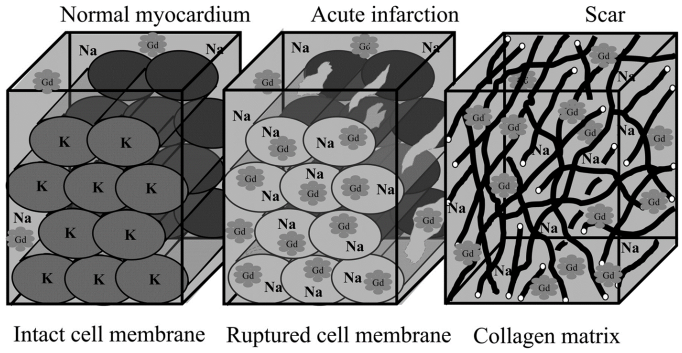

After intravenous administration the contrast diffuses to interstitial space. Within few minutes most of contrast diffuses to the blood to be excreted by kidney (the left image). In case of an ongoing myocyte necrosis the contrast accumulates also inside the myocytes. The greater amount of the contrast lead to an increased (enhanced) signal on T1-weighted imaging (the middle image). In a region with excessive interstitial fibrosis (i.e., scar) the large chelates of gadolinium remain entrapped in the fibrous matrix, from where they are wash-out in a much longer time. Therefore the regions with fibrosis remain brighter for a longer time (the right image). Adopted from Kim et al. (2000).

1.5.6 Increased left ventricular wall stress

Ventricular wall stress depends from the cavity volume, wall thickness and intraluminal pressures. Permanent increase in the LV wall stress parallels with the progression of the heart failure and unfavorable hemodynamic status. In individuals with DCM the increased LV wall (verified invasively) has been associated with presence of LGE (Alter et al. 2007). According to a hypothesis, in the overloaded LV the myocardium has increased metabolic needs, which in turn leads to relative ischemia, myocyte necrosis and eventually fibrotic scarring. LGE related to the hemodynamic stress has been also explained by capillary leakage and delayed wash-out of the contrast from the affected region. Typically, the LGE has a pattern of a thin mid-wall stripe in the inter-ventricular septum. The predominant septal and mid-wall localization in the LV suggests that this region is exposed to the highest mechanical forces.

1.6 CMR for detection of myocardial inflammation

Detection of myocardial inflammation by CMR is based on a complex evaluation of all the above described tissue parameters. Diagnostic cut-offs for the qunatitative measures have been established and validated against endomyocardial biopsy. Edema ratio of >1.9 is a sensitive and specific sign of acute myocarditis, though the finding is uncommon in chronic low-grade inflammation (Gutberlet et al. 2008). Early postcontrast increase in the LV signal intensity of >45 % or EGE >4.0 are also reliable markers of the acute myocarditis (Friedrich et al. 2009). Presence of LGE in an otherwise healthy individual with clinically suspected acute myocarditis reliably confirms the diagnosis. However, the sensitivity of LGE depends from the activity of the inflammation, time from the onset of the disease and associated LV function. In fact, while LGE has been reported in up to 84 % of patients with acute (days-to-weeks) myocarditis, it was present only in 27–44 % patients with chronic (>6 months) and less-acute ("borderline") myocarditis (Gutberlet et al. 2008, Friedrich et al. 2009).

1.7 CMR for prediction of the outcome of DCM

Reliable prediction of LVRR and future adverse events has important clinical implications in an individual with DCM, especially for the cost-effective use of implantable cardioverter-defibrillators and optimal timing of the referral for heart transplantation. CMR, by assessment of the myocardial tissue characteristics, could serve for estimation of the clinical course of the disease. Numerous studies

have demonstrated strong association between the presence of LGE and a poor outcome of DCM. However, the prognostic role of LGE was investigated mostly in the patients with chronic DCM (Bello et al. 2003).

Previously, only one study investigated predictive value of LGE in the specific population of the patients with new-onset DCM. But the study was undermined by the fact that the target endpoint was defined by a clinically somewhat irrelevant 5 % increase in LV ejection fraction (Leong et al. 2012). Therefore, the prognostic role of CMR in this subpopulation remains unclear. Of note, while in chronic DCM the LGE more likely reflects a definite fibrotic scar, in the new-onset DCM it could account as well for an active (and potentially reversible) myocardial injury.

1.8 Unresolved questions in the area of CMR in DCM

It can be concluded that CMR is reliable in detection of acute myocardial inflammation and somewhat less reliable in chronic myocardial inflammation. However, the diagnostic performance of CMR has been validated predominately on patients with clinically overt acute myocarditis who had preserved LV function (Table 2). Therefore it is not known whether the experience with the diagnosis of myocardial inflammation by CMR can be fully applied to the setting of DCM.

Table 2: An overview of studies on the use of CMR for detection of myocardial inflammation.

Publication	Year	Validation	Patients	Controls	LV dysfunction	Chronic myocarditis
Friedrich et al.	1998	clinical	19	18	−	−
Laissy et al.	2002	clinical	20	7	−	−
Rieker et al.	2002	clinical	11	10	−	−
Laissy et al.	2005	clinical	24	31	−	−
Abdel-Aty et al.	2005	clinical	25	22	−	−
Mahrholdt et al.	2006	histological	87	26	−	−
Gutberlet et al.	2008	histological	48	35	−	+
Yilmaz et al.	2008	histological	55	30	−	−
Ong et al.	2011	histological	16	19	−	−
Voigt et al.*	2011	histological	12	11	+	+
Mavrogeni et al.	2011	histological	85	20	−	−
Total			402	229		

* This was the only work that evaluated performance of CMR for diagnosis of chronic myocardial inflammation in the setting of DCM. Adopoted from Friedrich et al. (2009).

There is only a limited experience with interpretation of the CMR tissue imaging in the patients with new-onset DCM (Leong et al. 2012). In these patients, similar CMR findings may represent completely different pathophysiological processes. For example, LGE may reflect an active and potentially curable myocarditis, a permanent fibrotic scar or as well an ongoing myocardial necrosis related to the hemodynamic overload (Alter et al. 2007).

In the patients with chronic DCM or ischemic heart disease the finding of LGE usually remains permanent because it reflects a definite fibrotic scar. In contrast, in the patients with acute myocarditis and normal LV function the LGE may recede within several months, after healing of the inflammation (Friedrich et al. 1998). It is not known whether the LGE would recede also in the patients with new-onset DCM and whether it would be paralleled with LVRR.

At last, there is a sound evidence that in individuals with chronic idiopathic DCM the presence and extent of LGE projects poor clinical outcome (Bello et al. 2003). In contrast, only one study evaluated predictive value of LGE also in patients with new-onset DCM (Voigt et al. 2011). No data exists whether the LGE would also predict adverse clinical events in these patients and whether the LGE would outperform EMB, biomarkers or other conventional predictors.

2 Aims and hypotheses

Study aims:

1. To evaluate performance of CMR in detection of myocardial inflammation in the patients with new-onset DCM, using endomyocardial biopsy as a reference standard.
2. To clarify pathological and pathophysiological background of the CMR findings in these patients.
3. To evaluate value of the CMR findings for prediction of LVRR and adverse clinical events in these patients.

Hypotheses:

1. We expect that myocardial inflammation will be a common finding in the patients with recent-onset DCM.
2. Multisequential CMR imaging could detect the myocardial inflammation with an acceptable accuracy, provided that the inflammation would have certain minimal level of activity.
3. Pathophysiology of the CMR findings could be clarified by a simultaneous assessment by CMR, endomyocardial biopsy and specific cardiac biomarkers.
4. Some CMR findings might reflect myocardial inflammation but they could also reflect pathophysiological processes related to the heart failure itself.
5. We expect that LVRR would be a common phenomena in our patients. On the other hand, we expect also a number of severe adverse clinical events.
6. A greater extent of myocardial damage at baseline, as assessed by the LGE technique, could signify a worse chance for the LVRR and an increased risk of the adverse clinical events.
7. On the other hand, baseline presence of myocardial edema, assesed by T2-weighted imaging, and its regression during the follow-up could predict a better prognosis.

Rationale for the hypotheses:

Ad 1: Myocardial inflammation can be found in 27-52 % of individuals with DCM (Kawai 1999, Feldman & McNamara 2000). The prevalence of myocarditis in DCM depends to a great extent on the acuity of the clinical presentation and on the time of the imaging from the onset of the symptoms. Because the present study excludes chronic forms of DCM, the prevalence of myocarditis could be somewhat higher than in an unselected DCM patient population (Friedrich et al. 1998). On the other hand, it must be pointed out that the present study also excludes patients with clinically suspected myocarditis.

Ad 2: The diagnostic accuracy of CMR for detection of myocarditis may reach 68-78 % in the patients with clinically overt acute myocarditis (Friedrich et al. 2009). If the inflammation has a low activity, the pathological tissue processes (such as tissue edema, necrosis and fibrosis) may be smaller than is the detection capability of CMR (in terms of contrast-to-noise and voxel resolution) (De Cobelli et al. 2006).

Ad 3: Endomyocardial biopsy will enable to evaluate presence and activity of inflammatory cells, myocyte necrosis and extent of interstitial fibrosis (Cooper et al. 2007). B-type natriuretic peptide, which is synthesized in cardiomyocytes in response to increased wall stress and neurohormal activation, can be used as a surrogate of LV filling pressures (Schrier & Abraham 1999, Kazanegra et al. 2001). New-generation (high-sensitivity) cardiac troponin assays can detect ongoing myocyte necrosis on a submicroscopic level (Sherwood & Kristin Newby 2014). Combination of these methods could explain pathological and pathophysiological background of some of the CMR findings.

Ad 4: In patients with normal LV function, the finding of LGE is a sensitive and specific sign of myocardial inflammation (Friedrich et al. 1998). However in the patients with DCM the LGE could also reflect myocardial injury caused by relative regional ischemia due to hemodynamic overload (Alter et al. 2007). While the earlier can be detected by EMB the later can be evaluated by the assessment of cardiac troponins.

Ad 5: Previous studies reported LVRR at 12 months in 27 % to 56 % of patients with new-onset DCM, depending on the definition of DCM and on the therapy of heart failure (Steimle et al. 1994, McNamara et al. 2001, Binkley et al. 2012, Wilcox et al. 2012).The occurrence of LVRR negatively correlated with adverse clinical events (Merlo et al. 2011).

Ad 6: The LGE reflects active or healed myocardial injury. Studies in various pop-

ulations with DCM demonstrated association between LGE and a decreased chance for improvement of LV function and increased risk of adverse clinical events (Leong et al. 2012, Ismail et al. 2012, Gulati et al. 2013, Zagrosek et al. 2009)

Ad 7: Initial presence of myocardial edema and its regression during the follow up may reflect convalescence of initially acute myocarditis (Zagrosek et al. 2009), which in turn is usually associated with a good prognosis (Cooper 2009).

3 Methods

3.1 Study population

The study examined consecutive patients with DCM and a history of symptoms of heart failure shorter than 6 months. DCM was defined by established criteria as the presence of left ventricular (LV) dilatation (LV end diastolic diameter >33 mm/m in males and >32 mm/m in females) and LV systolic dysfunction (LV ejection fraction <45 %) in the absence of coronary artery disease, severe systemic arterial hypertension and primary valve disease (Lang et al. 2005, Maron et al. 2006).

Individuals with a history of drug abuse or excessive alcohol consumption, individuals presenting with persistent supraventricular tachyarrhythmias, individuals presenting with clinical signs suggestive of acute myocarditis (chest pain accompanied by characteristic abnormalities on ECG and significant increase in serum troponin) and individuals with a contraindication to CMR were excluded.

3.2 Study protocol

Initially, the patients were admitted to a specialized heart failure clinic. All of them underwent a thorough clinical assessment, ECG, echocardiography, CMR, EMB and cardiopulmonary exercise testing. Peripheral venous blood was obtained in the morning before EMB for the measurement of high-sensitivity troponin T (hs-cTNT), B-type natriuretic peptide (BNP), galectin-3, serum autoantibodies, and for routine biochemical analysis. EMB was performed within two days following the CMR. Patients admitted with decompensated heart failure were investigated only after achieving euvolemic state.

After discharge from hospital, the patients were followed during regular clinical visits at 3 and 6 months and every 6 months thereafter. The follow-up visits included clinical assessment, ECG, echocardiography, cardiopulmonary exercise testing, routine biochemical analysis and measurement of BNP. CMR was repeated also after 12 months of follow-up in all non-transplanted patients that did not have an implanted cardiac device. Pharmacotherapy of heart failure was optimized according to the contemporary guidelines (Dickstein et al. 2008).

Diagnosis of inflammatory DCM was established at baseline, after obtaining results of the EMB. LVRR was evaluated after 12 months of follow-up. A composite clinical endpoint of cardiac death, urgent heart transplantation and hospitalization for worsening of heart failure was recorded during the whole available follow-up.

3.3 Echocardiography

Echocardiography was performed by experienced operators in accordance with guidelines of the American Society of echocardiography (Lang et al. 2005, Quinones et al. 2002). M-mode, 2D images and Doppler recordings were obtained using a Vivid 7 (GE Healthcare, Chalfont St Giles, UK). LV ejection fraction was assessed using Simpson's biplane method. Mitral regurgitation was graded semi-quantitatively on a scale of none, trivial, mild, moderate and severe. Mitral inflow pattern was classified as restrictive in the presence of an E-wave deceleration time <120 ms or a ratio of early transmitral flow velocity to atrial flow velocity ≥ 2 associated with an E-wave deceleration time $\leq$150 ms (Nishimura & Tajik 1997). LVRR was defined as an absolute increase in LV ejection fraction $\geq$10 % to a final value of >35 %, and at the same time a decrease in LV end diastolic diameter $\geq$10 %.

3.4 Cardiopulmonary exercise testing

Cardiopulmonary exercise testing was performed using a symptom-limited bicycle ergometry and 25-watt increases in workload every 3 minutes. Minute ventilation, oxygen consumption, and carbon dioxide output were measured by a heated pneumotachograph and mass spectrometry (Sensormedics system, Viasys Healthcare Inc., Conshohocken, Pennsylvania, USA), as previously described (Kubanek et al. 2006).

3.5 Cardiac magnetic resonance imaging

CMR was performed on a 1.5 Tesla scanner (Avanto, Siemens Medical Solutions, Erlangen, Germany) equipped with a 12-channel body coil. The entire examination took about one hour, depending on the patient's cooperation and heart rate. Table 3 provides an overview of the used imaging sequences. All the images were acquired during breath-hold in inspiration.

Cine loops for quantification of cardiac volumes and function were obtained in standard short-axis and orthogonal long-axis cardiac planes using an ECG-gated steady-state free precision imaging sequence (True FISP). At least 25 phases were acquired per heartbeat, thus rendering a typical temporal resolution of 30–40 ms.

T2-weighted images for visualizing myocardial edema were acquired in short-axis at 1 cm intervals through the left ventricle using a dark blood sequence with suppression of fat (Fat SAT). The body coil was temporarily deactivated to avoid hardware-derived signal inhomogeneity.

Images for assessment of early enhancement were acquired using a T1-weighted fast low-angle sequence (Turbo FLASH). Three short-axis slices were obtained at basal, mid-papillary and apical level of the left ventricle. The images were acquired before and after 40–70 seconds after intravenous bolus injection of 0.2 mmol/kg of Gadobutrol (Gadovist, Bayer Schering, Germany).

Images for evaluation of late gadolinium enhancement were obtained 10 min after the administration of the contrast in short-axis and orthogonal long-axis planes using a 2D phase-sensitive inversion-recovery sequence. A typical scan time was 7–10 minutes. Triggering of the sequence was set to late systole to minimize motion-related artifacts. Inversion time was carefully selected on scout images to null the signal of the presumed normal myocardium. The field of view was adjusted to maximize spatial resolution. The number of lines in k-space and the triggering was adjusted according to the patient's heart rate to minimize motion artifacts.

Table 3: Typical parameters of the imaging sequences.

Sequence	Cine loops	T2	EGE	LGE
Repetition time (ms)	65	2 x RR	170	690 – 850
Echo time (ms)	1.2	58	1.02	3.2
Inversion time (ms)	–	140	100	230 - 300
Flip angle (°)	70	–	12	–
Field of view (mm)	240 x 260	290 x 380	300x 330	240 x 260
Matrix (pixels)	170 x 190	230 x 300	150 x 165	170 x 190
In-plane resolution (mm)	1.4 x 1.4	1.3 x 1.3	2.0 x 2.0	1.4 x 1.4
Slice thickness (mm)	8	8	10	8
Interslice gap (mm)	0	2	–	0.8

3.6 Analysis of CMR images

Analysis of the CMR scans was blinded to the patients' clinical data and to the results of endomyocardial biopsy. Cardiac volumes and function were evaluated using a dedicated software Segment version 1.8 (Medviso, Lund, Sweden). Myocardial edema index, myocardial EGE ratio and the extent of LGE were quantified using a custom-made program written in Matlab (Mathworks, Natick, MA, USA).

3.6.1 Ventricular morphology and function

Ventricular volumes, mass and ejection fractions were measured on the short-axis cine images. In each slice, the endomyocardial and epicardial contours of both ventricles were manually delineated at endsystole and enddiastole. Papillary muscles were excluded. Accuracy of the segmentation was simultaneously inspected on 2- and 4-chamber views (Figure 2). The cardiac phases were defined as the images containing the smallest and the largest ventricular cross-sectional area, respectively.

Endsystolic and enddiastolic ventricular cavity volumes were determined by summation of volumes of the endomyocardial discs. The software enabled to compensate the endsystolic volume for anterior movement of the mitral annulus. For this purpose, the distance of the mitral annular movement during systole was manually measured on a long-axis loop. The measured value was subtracted from the slice thickness of the most basal slice. Thus, only a fraction of the volume of the most basal slice was used for the final calculation of the endsystolic volume. At enddiastole, all the discs were used for the calculation. The volume of the ventricular myocardium was obtained by subtracting the epicardial and endocardial discs at enddiastole. The LV mass was derived by multiplying the myocardial volume by the specific density of myocardium (1.05 g/cm^3).

Figure 2: Evaluation of cardiac volumes and function by CMR

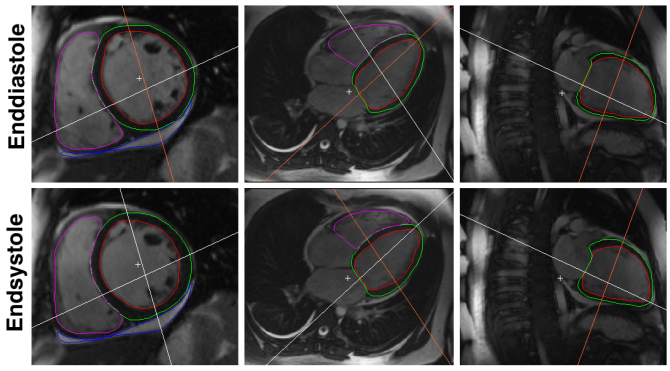

The figure demonstrates quantification of ventricular volumes and function in a patient with DCM. Contours of both ventricles were manually traced on each of the short-axis images (left panels) during enddiastole (top row) and endsystole (bottom row). Accurracy of the segmentation was veryfied on the long-axis views (middle and right panels).

3.6.2 Myocardial edema

Myocardial edema was evaluated on the T2-weighted short-axis images according to a previously described method (Friedrich et al. 2009). At first, 3–4 slices containing a cross-section through a paraspinal or a pectoral muscle were selected. The skeletal muscles were identified by side-by-side viewing of the T2-weighted images and the T1-weighted cine images. The left ventricular myocardium was manually delineated. Another region of interest with an area of 2–3 cm^2 was manually drawn over the skeletal muscle (Figure 3). For each slice, the myocardial edema index was calculated by dividing the mean signal intensity of the left ventricular myocardium by the mean signal intensity of the reference skeletal muscle. Global myocardial edema index was obtained by averaging the values from each of the slices. A higher value of the index reflected a greater myocardial water content. A value of $\geq$1.9 was regarded as abnormal (Friedrich et al. 2009).

Figure 3: Evaluation of myocardial edema by CMR

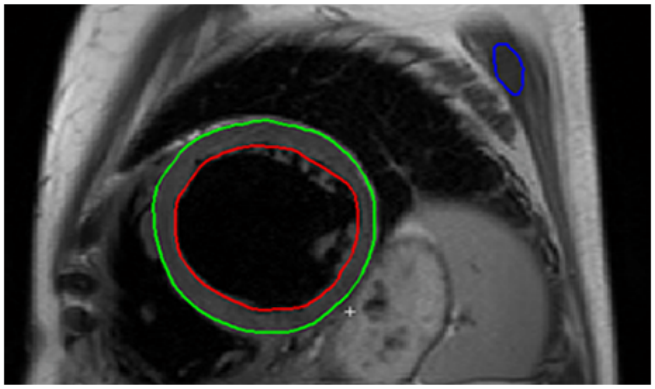

The figure demonstrates quantitative assesment of global left ventricular myocardial edema on a T2-weighted image. Myocardial edema index was calculated by dividing the mean signal of the left ventricular myocardium by the mean signal of a region of a refernce skeletal muscle in the view. Tissue containing a greater water content appeared brighter.

3.6.3 Pericardial effusion

Pericardial effusion was quantified by summation of volumes of manually delineated regions on the T1-weighted short-axis images. T2-weighted images were simultaneously reviewed to differentiate the effusion from epicardial fat. A total effusion volume of >50 ml was regarded pathological (Bogaert & Francone 2009).

3.6.4 Early gadolinium enhancement

Myocardial early enhancement was quantified on the Turbo FLASH images according to the method by Laissy et al. (2005). Similarly as for the myocardial edema index, the left ventricular myocardium and a skeletal muscle in the view were manually segmented on the pre- and postcontrast images (Figure 4). Myocardial relative enhancement was calculated by the formula: mean postcontrast signal – mean precontrast signal / mean precontrast signal. The same formula was applied for calculating relative enhancement of the reference skeletal muscle. The myocardial early enhancement ratio was obtained by dividing the relative myocardial enhancement by the relative skeletal muscle enhancement. Value from all the three slices were averaged to obtain the myocardial global early gadolinium enhancement ratio (EGE). A value of $\geq$45 % was regarded abnormal (Laissy et al. 2002).

Figure 4: Assessment of myocardial early gadolinium enhancement ratio

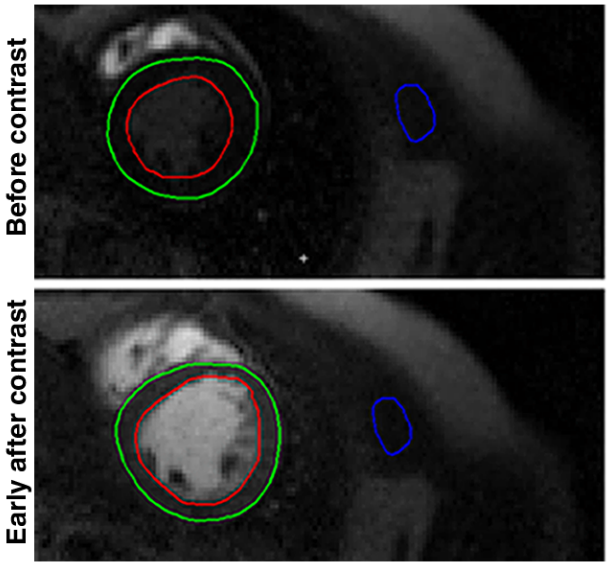

The figure demonstrates quantification of EGE ratio. Left ventricular myocardium and a reference skeletal muscle in the view were manually delineated on a precontrast and a postcontrast image. The mean singal intestities of the segmented regions were used for the calculation of the relative enhancement.

3.6.5 Late gadolinium enhancement

The presence of late gadolinium enhancement (LGE) and its localization in the left ventricle were independently determined by two expert radiologists. The LGE had to be visible in phase-sensitive and also in magnitude-reconstructed sequences.

Any LGE finding in the short-axis view had to be confirmed in an orthogonal long axis view through the lesion.

The extent of LGE in the left ventricle was quantified on the short-axis images by a semiautomatic algorithm adopted from Heiberg et al. (2005). The left ventricular myocardium was segmented manually. In each slice the program automatically delineated a region in the left ventricular wall that contained an intersection of a 15 degree sector of the wall and the central 80 % of the wall thickness. Mean signal intensity of the region was recorded. This process was repeated iteratively by one degree steps until the whole left ventricular wall was encircled. The region with the lowest mean signal intensity was set as a reference tissue. Myocardial tissue with signal intensity >2 standard deviations above the mean of the reference myocardium was regarded as abnormally enhanced (Kim et al. 1999). Isolated regions of LGE that were smaller than 1.5 ml were regarded as artefacts and they were automatically removed. The extent of LGE was expressed as a weight of tissue and also as a percentage of left ventricular mass (indexed LGE extent). Figure 5 demonstrates the process of the quantification of the extent of LGE. Another example is shown on the Figure 12 (page 50).

Figure 5: Quantification of the extent of LGE

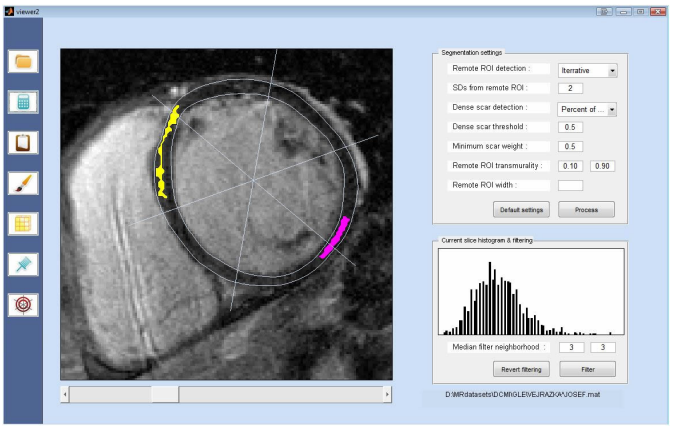

The figure shows a custom-made program for semiautomatic quantification of the extent of LGE in the left ventricle. The LGE is quantified slice-by-slice and summed for the whole ventricle. The program automatically identifies a region of a predefined size with the lowest signal intensity (depicted by pink color on the figure). This region is classified as a reference "healthy" myocardium. The LGE is outlined automatically by applying a threshold of 2 standard deviations above the mean signal intensity of the reference myocardium (depicted by yellow color). Artifacts can be removed by adjusting a minimum LGE weight (in grams) or minimum LGE area (in pixels). To improve homogeneity of the image, the program allows also median image filtering with an adjustable size of the kernel.

3.7 Assessment of cardiac biomarkers

Plasma levels of BNP were measured immediately after blood sampling using a commercially available electrochemiluminescent immunoassay (Architect BNP, Abbott Diagnostics, Illinois, U.S.A.). The lower limit of detection was 10 ng/L; intra- and inter-assay coefficient of variation (CV) was 3.8 % and 5.3 %. Serum for assessment of hs-cTnT was frozen at −30°C until batch analysis. Hs-TnT was measured by an electrochemiluminescent immunoassay (T-hs-STAT, Cobas e411, Roche Diagnostics GmbH, Mannheim, Germany). The lower limit of detection was 5 ng/L; CV at 13 ng/L was 10 %, intra- and inter-assay CV was 3.2 % and 6.2 %. The upper reference limit was set at 13.5 ng/L. Glomerular filtration rate was estimated using the Modification of Diet in Renal Disease (MDRD) formula (Levey et al. 1999).

3.8 Endomyocardial biopsy

Endomyocardial biopsy was performed under fluoroscopic guidance via the right internal jugular vein using a flexible bioptome (diameter 7F, Cordis Europe, Netherlands). Myocardial specimens were harvested from the right ventricular side of the interventricular septum. There were no complications related to the procedure.

At least four samples were fixed in 4 % buffered formaldehyde for histopathological and immunohistochemical analysis. Another three samples were placed under aseptic conditions into ice-cold sterile saline and immediately transferred into the microbiological laboratory for detection of viral genome.

3.8.1 Histopathological analysis

Light microscopy was performed on 4-µm-thick sections from paraffin-embedded endomyocardial biopsy specimens stained with hematoxylin-eosin, periodic acid-Schiff, elastic picro-sirius red and Masson's trichrome. Histopathological analysis followed the Dallas criteria (Aretz et al. 1987). Active myocarditis was defined by the finding lymphocytic infiltrates associated with myocyte necrosis. Finding of inflammatory infiltrates but without signs of myocyte injury was classified as borderline myocarditis.

The extent of interstitial fibrosis was evaluated on the picrosirius-stained slides by a morphometric study as described by Loud & Anversa (1984). At least three representative microscopic fields (enlargement of 400 x) were analyzed in each biopsy specimen. Each microscopic field was superimposed by a grid of 100 in-

tersection points. The points overlying red-colored (fibrotic) tissue were counted. To calculate the percentage of interstitial fibrosis, the sum of the counted fibrotic points from all the fields were divided by the total number of points in the fields. Areas containing artifacts or perivascular fibrosis were excluded from the calculation.

Myocyte vacuolization (a sign of the myocyte degeneration) was graded on a semiquantitative scale: 1 = no or scarce vacuolization, 2 = focal vacuolization, 3 = extensive vacuolization.

3.8.2 Immunohistochemical analysis

CD3 and CD68 and positive cells were detected on 4 µm-thick paraffin sections of the biopsy samples using a two-step indirect method. The slides were deparaffinized in xylene, rehydrated in graded ethanol and heated in 0.01M citrate buffer pH 6.0 (detection of CD68) and EDTA buffer pH 8,0 (detection of CD3) for target retrieval. Endogenous peroxidase was blocked by 0.3 % H2O2 in 70 % methanol for 30 minutes. The primary antibodies (both from Dako, Glostrup, Denmark) were applied for 30 minutes. They were detected by polymer Histofine Simple Stain MAX PO (Nichirei, Japan). Finally, the specimens were covered for 5 minutes with Dako Liquid DAB+ Substrate-Chromogen System (Dako, Glostrup, Denmark), counterstained with Harris's hematoxylin (Merck, Germany) and embedded in Entellan (Merck, Germany).

Immunohistochemical criteria of myocardial inflammation were based on detection of mononuclear infiltrates: either >7 per mm^2 of CD3 postitive T-lymphocytes or a combination of >14 per mm^2 of CD3 positive T-lymphocytes or CD68 positive macrophages (Richardson et al. 1996).

3.8.3 Detection of viruses in the myocardium

Isolates from the EMB specimens were used to detect the following viruses: human cytomegalovirus, Epstein- Barr virus, human herpes virus 6, parvovirus B19, adenoviruses and enteroviruses (including coxackieviruses and echoviruses). Nucleic acids were isolated with QIAamp DNA Mini Kit (Qiagen Gmbh, Hilden, Germany) and RTP DNA/RNA Virus Mini Kit (Invitec, Berlin, Germany) according to the protocol for purification of nucleic acids from tissues. Cytomegalovirus was detected by an in-house assay as reported previously (Pumannova et al. 2006). The remaining viruses were analyzed using commercially available assays: LightMix EBV Kit and LightMix HHV-6 Kit (both from TIB MOLBIOL Gmbh, Germany), LightCycler Parvovirus B19 Quantification Kit (Roche Diagnostics, USA), Aden-

ovirus R-Gene Kit (Argene, Verniolle, France) and Enterovirus R-Gene Real-Time Kit (Argene, Verniolle, France).

3.9 Ethics

The investigation conformed to the principles outlined in the Declaration of Helsinki (WMA 2004). It was approved by the institutional ethics committee. All subjects signed an informed consent prior to their participation in the study.

3.10 Statistical analysis and data reporting

All statistical analyzes were conducted with SPSS version 17.0 (SPSS, Chicago, IL). P <0.05 was considered to be statistically significant.

Values are reported as frequency (percentage), mean $\pm$ standard deviation or median [interquartile range].

Categorical variables were compared using the chi-square or Fisher's exact test. Continuous variables were compared by the Student's t-tests or by the Mann-Whitney U test, as appropriate. Because of right-skewed distribution, the concentrations of BNP and hs-TnT were log-transformed before analysis.

To identify independent factors associated with myocardial inflammation, LVRR and presence of LGE, variables that significantly differed in the univariate between-group analyzes were entered into a multiple stepwise logistic regression analysis. Predictive performance of the selected variables was assessed using receiver operator characteristics (ROC) analysis. Log-rank test and Cox's proportional hazard model, using the time to first event, were performed to analyze associations between the variables of interest and the composite end point of adverse clinical events.

4 Results

4.1 Study population

A total of 44 Caucasians with new-onset DCM were investigated. Two of the patients were excluded from the head-to-head comparison of CMR and EMB because of poor image quality of the EGE sequence. For the evaluation of LVRR, all the 44 patients had complete clinical, laboratory, echocardiography and biopsy data, along with CMR-derived ventricular volumes and function, LGE sequences and T2-weighted sequences. Baseline clinical characteristic of the study population are summarized in Table 4.

4.2 Clinical characteristics of patients with new-onset DCM

A typical patient with new-onset DCM was a middle-aged man without a previous medical history. None of the patients had a history of coronary artery disease, peripheral arterial disease or stroke. Only two individuals were treated for diabetes mellitus, but in both cases it was adequately controlled only by oral antidiabetics. Three patients were treated for arterial hypertension; they had normal blood pressure on medication. All but one patient had initially sinus rhythm. One patient presented with persistent atrial fibrillation but she did not have an excessive heart rate. After performing electric cardioversion he remained in sinus rhythm for the rest of the follow-up.

Importantly, none of the patients presented with a clinical picture that would suggest an acute myocarditis (chest pain, marked elevation of cardiac troponin, characteristic abnormalities on electrocardiography or an audible pericardial friction rub). In contrast, about every forth patient reported typical symptoms of a viral respiratory disease occurring a few weeks before onset of the symptoms of heart failure. Also, interestingly, every fourth patient reported a family history of a cardiomyopathy in at least one of his first-degree relatives.

Before the baseline evaluation, the patients had been suffering from symptoms of heart failure for median 2 months (minimum 2 weeks, maximum 6 months). The most typical complaints included exertional dyspnea, markedly lowered tolerance of physical activity or ankle swelling. At the time of their first medical contact two thirds of the patients had to be hospitalized for decompensated heart failure.

Initially, the patients were usually treated at a regional community hospital before they were referred to our center for further investigation and treatment. At the time of admission to our center 68 % were hemodynamically stable, 18 %

Table 4: Baseline characteristics of the study population.

Variable	n = 44
Clinical variables	
Age (years)	43 ± 11
Males	31 (71 %)
Family history of dilated cardiomyopathy	11 (25 %)
Diabetes mellitus	2 (4 %)
Systemic hypertension	3 (7 %)
Viral prodromes during preceeding month	12 (27 %)
Duration of symptoms of heart failure (months)	2.0 [1.0–3.4]
Hospitalisation for heart failure in previous 6 months	29 (66 %)
Decompensated heart failure at admission	14 (32 %)
NYHA class	
I	1 (2 %)
II	23 (52 %)
III	14 (32 %)
IV	6 (14 %)
Body mass index (kg/m^2)	25 ± 4
Systolic blood pressure (mm Hg)	112 ± 17
Diastolic blood pressure (mm Hg)	69 ± 7
Heart rate (beats/min)	84 ± 18
Sinus rhythm	43 (98 %)
QRS duration (ms)	106 ± 21
Complete left bundle branch block	5 (11 %)
Exercise capacity*	
Peak exercise heart rate (beats/min)	142 ± 17
Peak exercise systolic BP (mm Hg)	135 ± 22
Peak oxygen consumption (ml kg/min)	19.4 ± 0.5
Peak oxygen consumption (% of predicted value)	57 ± 16
VE/VCO2 slope	28.8 ± 0.9
Biomarker testing	
Sodium (mmol/l)	141 ± 2
Creatinine (µmol/l)	95 ± 4
Estimated glomerular filtration rate (ml/min)	79 ± 23
B-type natriuretic peptide (ng/l)	635 [276–1081]
High-sensitivity troponin T (ng/l)	14.5 (5.0–30.0)
High-sensitivity troponin T positive†	23 (52 %)
Conventional troponin I positive†	13 (29 %)
Galectin-3 (µg/l)	3.0 [0.2–4.6]
C-reactive protein (mg/l)	3.0 [1.0–8.2]

* Available in 41 patients; † Troponin positivity was defined as high-sensitivity troponin T >13.5 ng/l or conventional troponin I >0.03 µg/l.

had decompensated heart failure that did not require treatment with inotropes and another 14 % had decompensated heart failure requiring treatment with inotropes. The patients presented mostly with NYHA II functional class (52 %), followed by NYHA III (32 %), NYHA IV (14 %) and NYHA I functional class (2 %). Table 5 shows an overview of the patients' medication at the time of the CMR during the index hospitalization.

After admission to our center, the patients with decompensated heart failure were first managed by diuretics and, if necessary, by inotropes to achieve an euvolemic state. This phase usually took 1-2 weeks. CMR, EMB and blood sampling for assessment of cardiac biomarkers was performed (if possible) only after the initial compensation. Functional exercise testing was performed only in hemodynamically stable individuals before a planned discharge to home.

Table 5: Baseline pharmacotherapy of heart failure.

Medication class	n = 44
ACEI/ARB	40 (91 %)
ACEI or ARB $\geq$ 50 % of maxinum recommended dose	10 (23 %)
Beta-blockers	41 (93 %)
Beta-blockers $\geq$ 50 % of maximum recommended dose	11 (25 %)
Furosemide	40 (91 %)
Furosemide $\geq$ 40 mg/day	30 (68 %)
Spironolactone	35 (80 %)
Intravenous furosemide or spironolactone	13 (29 %)
Inotropes*	6 (14 %)

* The inotropes consisted of low dose of dobutamine in five patients and dopamine in an another patient.

4.3 Baseline cardiac function

Key parameters of the patients' baseline cardiac function, as assessed by echocardiography and CMR, are summarized in Table 6. As a rule, the patients had dilated left ventricle (LV) with severely impaired systolic function. The mean LV fraction was 21 $\pm$ 10 % by echocardiography and 23 $\pm$ 7 % by CMR (range, 8–41 %). The average volume of the LV was 280 $\pm$ 85 ml, ranging from 117 ml up to 548 ml; mean LV enddiastolic diameter was 67 $\pm$ 7 mm (range, 48–83 mm). LV systolic dysfunction was often paralleled by systolic dysfunction of the right ventricle.

Importantly, as much as 39 % of the patients had also severely impaired left ventricular diastolic filling, which was reflected by a restrictive pattern of LV filling on Doppler echocardiography. Furthermore, more than a half of the patients had at least moderate functional mitral regurgitation, which was usually accompanied by dilated left atrium and signs of pulmonary hypertension.

Baseline exercise testing was performed in 41 (93 %) of the patients. Three patients were unable to perform the exercise testing because they remained hemodynamically unstable. As expected, the patients with recent-onset DCM showed markedly reduced exercise tolerance: VO_2 max was 57 ± 16 % of the expected values in healthy population matched for age and gender.

Table 6: Baseline assessment of cardiac morphology and function.

Variable	n = 44
Echocardiography	
LV enddiastolic diameter (mm)	69 ± 6
LV enddiatstolic diameter index (mm/m)	39 ± 3
Interventricular septum thickness (mm)	9 ± 1
Posterior wall thickness (mm)	8 ± 1
LV ejection fraction (%)	23 ± 7
Restrictive pattern of mitral inflow	17 (39 %)
E/E' ratio	13.2 ± 0.5
Left atrial short axis diameter index (mm/m)	26 ± 4
Left atrial volume index (ml/m^2)	49 ± 19
Mitral regurgitation mdrate or severe	25 (57 %)
RV enddiastolic diameter (mm)	29 ± 6
TAPSE (mm)	17 ± 5
Magnetic resonance imaging	
LV enddiastolic volume (ml)	280 ± 85
LV enddiastolic volume index (ml/m^2)	140 ± 40
LV ejection fraction (%)	21 ± 10
LV ejection fraction category	
< 20 %	15 (34 %)
20–24 %	16 (36 %)
25–29 %	7 (16 %)
30–34 %	3 (7 %)
35–45 %	3 (7 %)
LV mass (g/m^2)	105 ± 26
RV enddiastolic volume index (mL/m^2)	77 ± 30
RV ejection fraction (%)	24 ± 8

4.4 Findings in endomyocardial biopsy

The findings in the endomyocardial biopsy are summarized in Table 7. Figure 7 shows several representative images from the histological and immunohistochemical analysis. Immunohistochemical analysis of the endomyocardial biopsy specimens revealed myocardial inflammation in 15 individuals. The classical Dallas (histological) criteria of myocarditis were met only in three of the cases, but even in these three individuals the inflammation was classified as borderline.

In summary, 34 % patients had inflammatory DCM. Of them 7 % had borderline myocarditis according to Dallas criteria and 27 % had low-activity myocardial inflammation detected only by immunohistochemistry (but not by histopathology). The remaining 66 % of patients were concluded to have an idiopathic DCM (Figure 6).

Figure 6: Diagnoses based on the endomyocardial biopsy findings

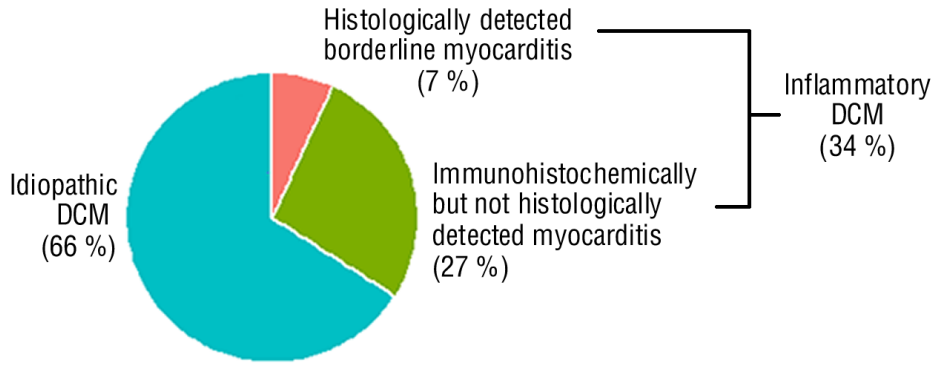

In the patients with myocarditis, the mean count of CD3+ T lymphocytes and CD68+ macrophages was 12 ± 5 and 8 ± 4 per mm^2, respectively. Two thirds of the patients had present at least one virus genome in the biopsy specimens. The most common genome found was parvovirus B19, followed by human cytomegalovirus and one case of enterovirus (Table 7). Human herpes virus 6 and adenoviruses were not found in any of samples.

Some degree of myocardial interstitial fibrosis was present in all the patients. The mean extent of fibrosis was 15 ± 5 %. There was no difference in the extent of myocardial fibrosis with respect to the presence of myocardial inflammation.

Figure 7: Typical findings in histological and immunohistochemical analysis

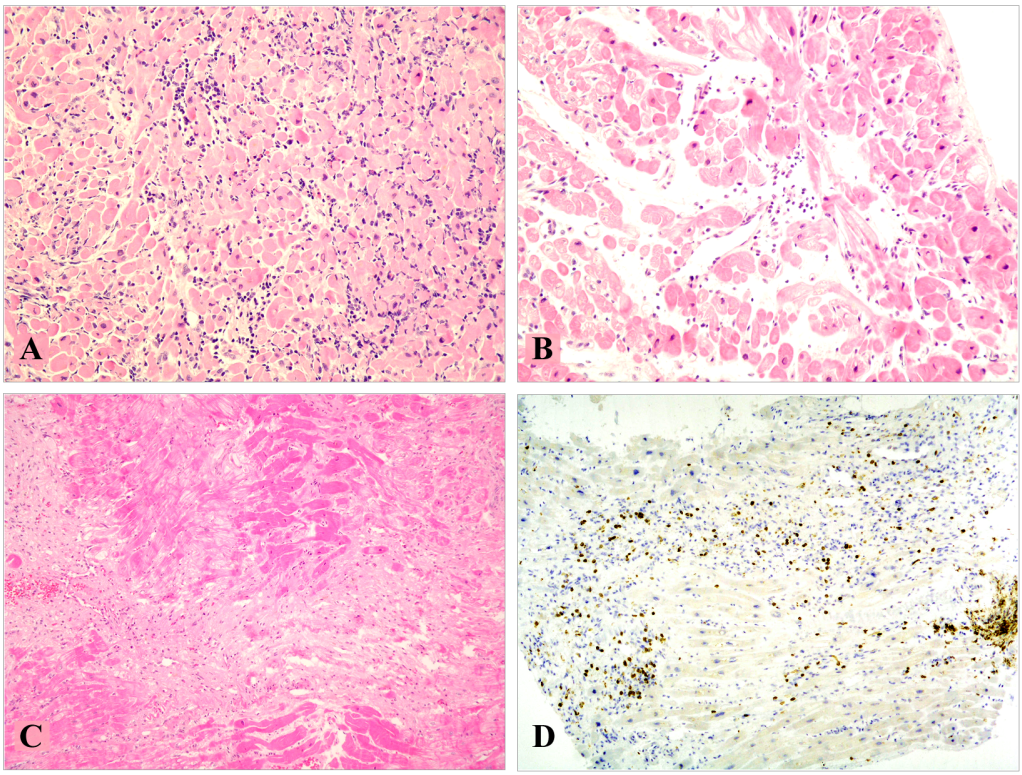

Panel A: Hematoxylin-eosin (HE) staining, zoom 200x. The image shows an acute myocarditis with diffuse lymphocytic infiltrate and focal necrosis of myocytes. This specimen was obtained in a patient with fulminant myocarditis who was not involved in this study.
Panel B: HE staining, zoom 200x. The image shows a borderline myocarditis with a more subtle lymphocytic infiltrate but no signs of myocytic degeneration or necrosis.
Panel C: HE staining, zoom 10x. The image shows borderline myocarditis with lymphocytic infiltration, which is accompanied by extensive interstitial replacement fibrosis.
Paned D: Immunohistochemical analysis with antibodies targeting CD3 antigens, zoom 10x. The image illustrates findings in individuals with a positive immunohistochemistry detecting inflammation. The brown dots represent CD3 positive T-lymphocytes.

Table 7: Findings in the endomyocardial biopsy.

Variable	n = 44
Area of available biopsy specimen (mm^2)	6 ± 2
Myocardial inflammation*	15 (34 %)
Myocardial inflammation by immunohistochemistry†	12 (27 %)
Borderline myocarditis by histological criteria‡	3 (7 %)
CD3+ T lymphocytes (n/mm2)	4 [2–9]
CD68+ macrophages (n/mm2)	2 [0–5]
Presence of virus genome	29 (66 %)
Parvovirus B19 positive	27 (61 %)
Parvovirus B19 in EMB (copies/µgof DNA)	120 [0–622]
Human cytomegalovirus	4 (9 %)
Enterovirus	1 (2 %)
Human herpes virus 6	0 (0 %)
Adenoviruses	0 (0 %)
Extent of myocardial fibrosis (%)	15 ± 5
Degree of myocyte vacuolization (grades 1–3)§	2 [2–3]

∗ Presence of $> 7\,/mm^2$ of CD3+ T-lymphocytes or a combination of $> 14\,/mm^2$ of CD3+ T-lymphocytes or CD68+ macrophages. † Immunohistochemical proof of myocardial inflammation but no signs of myocyte necrosis on histopathological assessment. ‡ Immunohistochemical and histopathological signs of myocardial inflammation with associated myocyte necrosis. § Grade 1 signifies absent or scarce vacuolization; grade 2, focal vacuolization and grade 3, extensive vacuolization or apoptosis.

4.5 Feasibility of CMR for assessing myocardial tissue characteristics

The image quality was good or acceptable in all but two individuals, in whom the scans were uninterpretable for evaluation of EGE ratio. In one case, the poor image quality was caused by heart motion artifacts; in the other case it resulted from an inappropriately selected inversion time. The sequences for evaluation of LGE and the myocardial edema ratio were interpretable in all cases.

There was a good agreement on the presence of LGE between the two raters (Kappa = 0.75, 95 % CI [0.53, 0.97], P = 0.001). Also, there was an excellent inter-observer reproducibility of the measurements of the quantitative parameters (extent of LGE, myocardial edema ratio and early enhancement). The relative variability of the measurement at a repeated analysis after three months was for extent LGE, 5.2 ± 4.5 %; for myocardial edema ratio, 6.9 ± 6.8 %; and for early myocardial enhancement, 10.1 ± 7.3 %. The biases and the limits of agreement for the repeated measurements of the quantitative tissue parameters are shown in the Blant-Altman plot on the Figure 8.

Figure 8: Reproducibility of the CMR quantitative tissue parameters

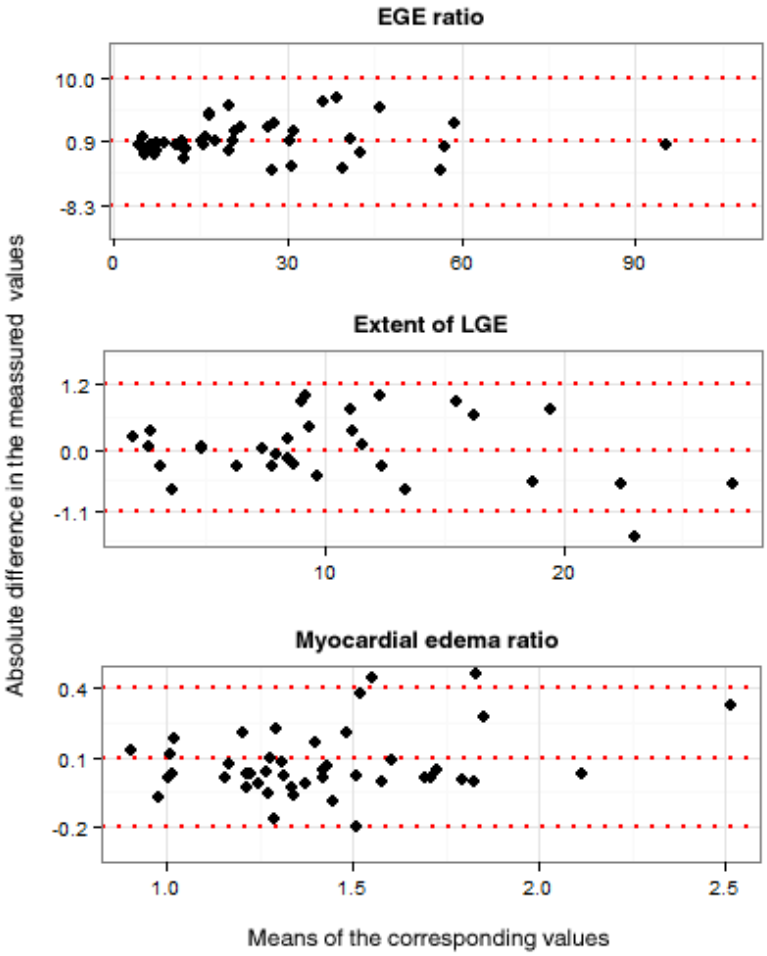

The red dotted lines represent the bias and limits of agreement at the 95 % confidence interval.

4.6 Accuracy of CMR for detection of myocardial inflammation

Tables 8 and 9 present comparison of clinical and CMR variables between patients with and without myocardial inflammation. A receiver-operator curve analysis of the diagnostic performance of the quantitative CMR parameters (myocardial edema ratio, EGE ratio and extent of LGE) for detection of myocardial inflammation is presented in Figure 9. The overall diagnostic performance of CMR for detection of myocardial inflammation is presented in Table 10.

The groups did not differ in the volume, mass or systolic function of the ventricles. Also, the two groups did not differ in the myocardial edema ratio. Consequently, the edema ratio proved insufficient for detection of myocarditis in DCM.

EGE was significantly increased in the patients with inflammatory DCM compared the idiopathic DCM. The parameter retained its independent predictive value also in a multivariate logistic regression analysis (Table 10). However, a receiver-operating characteristic analysis revealed only a modest diagnostic performance of this CMR sign (Figure 9). Moreover, the finding of an abnormally increased EGE ratio above the arbitrary cut-off of 45 % was rather uncommon in our study population (it was present only in 6 cases of inflammatory DCM and in 1 case of idiopathic DCM). Thus, while this CMR sing was highly specific it had a low sensitivity for detection of myocardial inflammation.

Table 8: Comparison of clinical, laboratory and biopsy data between individuals with idiopathic and inflammatory DCM.

Variable	Idiopathic DCM n = 27	Inflammatory DCM n = 15	p Value
Age (years)	45 ± 12	42 ± 8	0.29
Males	19 (70 %)	11 (73 %)	0.81
Duration of heart failure (months)	2 [1–3]	2 [1–3]	0.58
Prodromes of viral disease*	5 (19 %)	6 (40 %)	0.13
NYHA class	2.4 ± 0.9	2.8 ± 0.8	0.23
Diabetes mellitus	1 (4 %)	1 (7 %)	0.66
Systemic hypertension	2 (7 %)	1 (7 %)	0.93
GFR (ml/min/m^2)	81 ± 23	79 ± 15	0.69
ACEI/ARB	24 (89 %)	14 (93 %)	0.64
Beta-blockers	5 (19 %)	4 (27 %)	0.54
Furosemide	24 (89 %)	14 (93 %)	0.66
Spironolactone	20 (74 %)	13 (87 %)	0.34
Normal sinus rhytm	26 (96 %)	15 (100 %)	0.45
Left bundle-branch block	3 (11 %)	2 (13 %)	0.83
Hs-TnT (ng L)	11 [5–32]	17 [5–30]	0.55
Hs-TnT positive†	12 (44 %)	10 (67 %)	0.20
Troponin I maximum (µg/L)	1.6	1.7	—
Conventional troponin I positive†	7 (26 %)	6 (40 %)	0.34
C-reactive protein (mg/L)	2 [1–7]	3 [2–9]	0.36
B-type natriuretic peptide (ng/L)	963 [240–1508]	647 [279–1180]	0.27
Viral genome in biopsy	16 (59 %)	11 (73 %)	0.36
Extent of fibrosis in biopsy (%)	14 ± 7	15 ± 9	0.61

* Prodromes of a viral disease during the preceding month before onset of the symptoms of heart failure. † Hs-TnT >13.5 ng/l or conventional troponin I >0.03 µg/l.

Table 9: Comparison of CMR findings between the patients with idiopathic and inflammatory DCM.

Variable	Idiopathic DCM n = 27	Inflammatory DCM n = 15	p Value
LV enddiastolic diameter (mm)	67 ± 8	71 ± 7	0.14
LV mass (g/m^2)	106 ± 26	106 ± 27	0.96
RV ejection fraction (%)	24 ± 9	23 ± 8	0.64
RV enddiastolic volume (ml/m^2)	80 ± 35	76 ± 23	0.71
Interventricular septum (mm)	9 ± 2	9 ± 2	0.45
Edema ratio	1.5 ± 0.3	1.5 ± 0.4	0.67
Edema ratio > 1.9	2 (7 %)	2 (13 %)	0.63
EGE present	22 ± 13	38 ± 32	0.030*
EGE > 45 %	1 (4 %)	6 (40 %)	0.005*
LGE present	15 (56 %)	13 (87 %)	0.049*
Extent of LGE† (% of LV mass)	6 ± 4	5 ± 3	0.625
LGE mid-wall stripe pattern	11 (41 %)	9 (60 %)	0.23
Pericardial effusion > 50 ml	3 (11 %)	7 (47 %)	0.020*

* The symbol highlights a p-value <0.05. † Only in those with present LGE.

Table 10: Performance of CMR in detection of myocardial inflammation in DCM

Variable	Sensitivity	Specificity	Accuracy	OR [95% CI]
Myocardial edema*	13 %	93 %	64 %	NS
Increased EGE†	40 %	96 %	76 %	17 [2–164]
LGE present	87 %	44 %	60 %	5 [1–28]
Pericardial effusion‡	47 %	89 %	74 %	7 [1.5–34]
Any two criteria simultaneously	67 %	85 %	79 %	12 [3–52]
LGE + increased EGE	86 %	74 %	76 %	17 [2–164]
LGE + pericardial effusion	70 %	75 %	74 %	7 [1.5–37]

NS signifies statistically not significant by logistic regression. OR = odds ratio; CI = confidence interval; * Edema ratio >1.9; † EGE > 45 %; ‡ Pericardial effusion > 50 ml

Figure 9: Performance of the individual quantitative CMR tissue parameters in the detection of myocardial inflammation

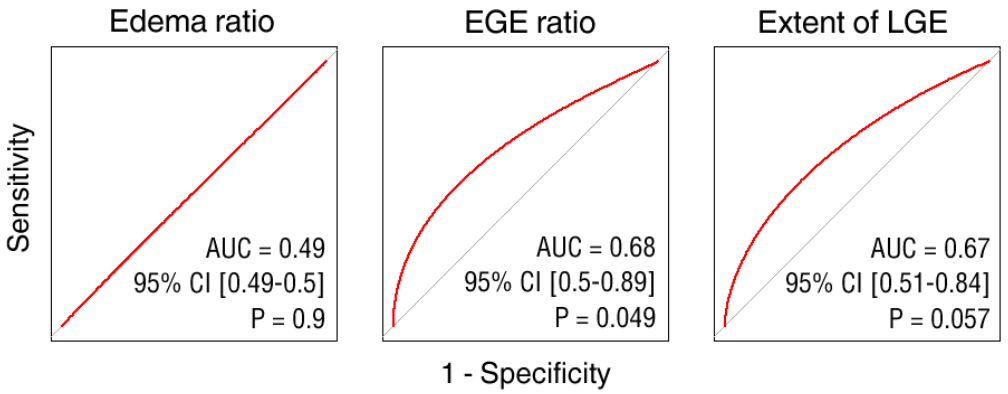

The figure shows a ROC analysis of three quantitative CMR tissue parameters for detecting myocardial inflammation in new-onset DCM. The myocardial edema ratio performed poorly (left plot). Early enhancement ratio showed only a modest diagnostic performance (middle plot). Quantification of the extent of LGE (right plot) did not add any diagnostic value compared to a simple binary statement of the presence LGE.

Similarly, an abnormal pericardial effusion (>50 ml) was quite uncommon in the patients with new-onset DCM but it was more frequent in inflammatory compared with idiopathic DCM. In a multivariate regression analysis, the finding of an abnormal pericardial effusion was an independent predictor of myocardial inflammation (Table 10). Of note, the effusion did not cause any hemodynamic compromise to the patients because it was never of a large volume (mean volume, 76 ml, range 52–185 ml).

LGE was present in 67 % of the study group. It was significantly more prevalent in the patients with inflammatory DCM. In the multivariate regression analysis, the finding of LGE was an independent predictor the myocardial inflammation (Table 10). Quantification of the extent of LGE did not improve the diagnosis compared to a simple binary classification of its occurrence in the LV (Figure 9).

The LGE had a pattern of a single, thin, mid-wall stripe located in the interventricular septum (n = 12) or within inferolateral or lateral wall (n = 4), multiple mid-wall stripes located in different areas (n = 7) or a patchy transmural lesion found predominantly in lateral wall (n = 5, Figure 10). We did not observe any characteristic pattern or a typical localization of the LGE that would reliably identify the individuals with myocardial inflammation (interventricular septum [Figure 10 A–B] vs. nonseptal regions [Figure 10 C–D]; 16 of 28 [50 %] vs. 12 of 28 [42 %], respectively; P = 0.66). Moreover, no characteristic localizations or patterns of LGE were observed with regard to a particular viral genome.

In summary, the diagnostic performance of CMR was suboptimal for clinical application. LGE was sensitive but not specific for myocardial inflammation, while abnormal pericardial effusion and increased EGE ratio turned to be specific but less sensitive findings. In fact, the most accurate diagnostic approach was achieved if the CMR criteria for myocardial inflammation was defined as the simultaneous presence of any two of the above three CMR signs.

Figure 10: Examples of LGE in the patients with new-onset DCM

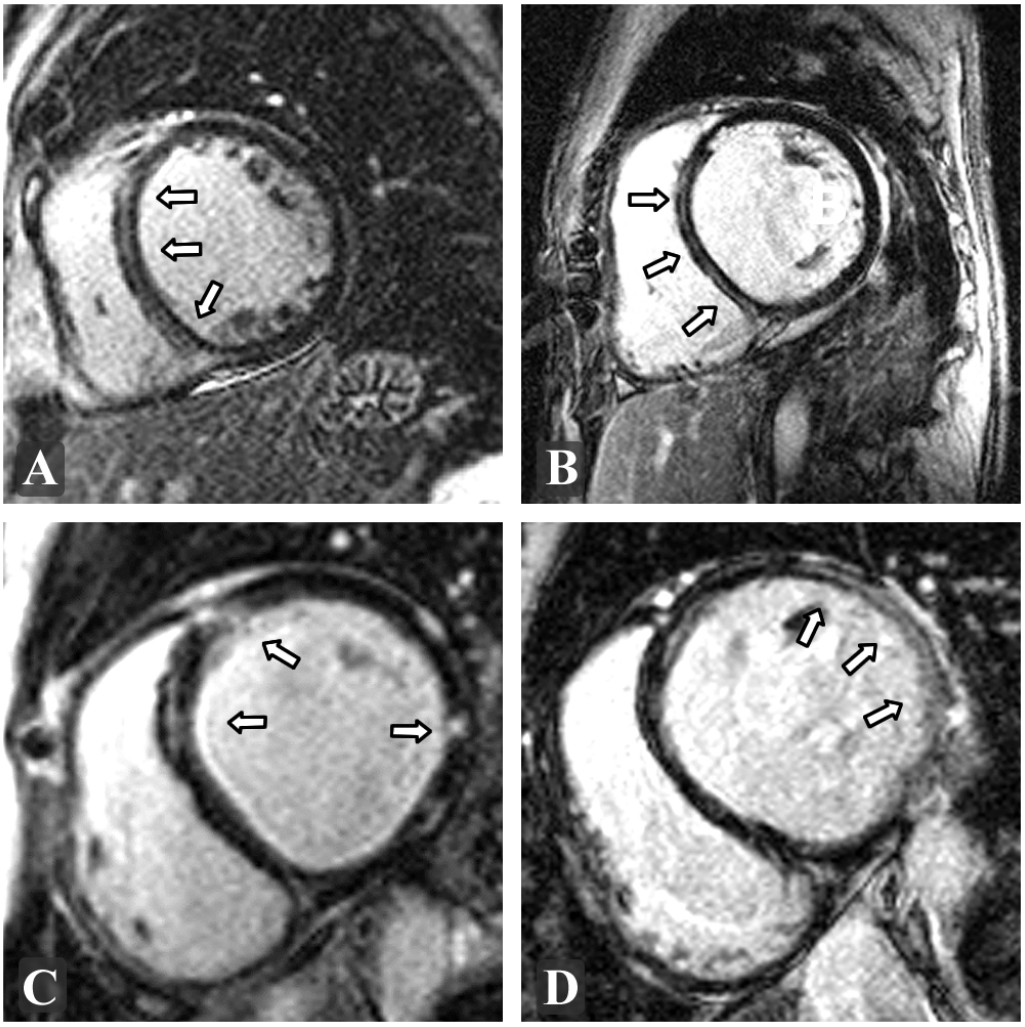

The figure illustrates various typical patterns of LGE which can be found in individuals with new-onset DCM.
Panels A and B: a thin mid-wall stripe located in the interventricular septum.
Panel C: multiple patches of LGE located in the LV septum and also in the LV free wall.
Panel D: extensive transmural LGE in the LV free wall.

4.7 Pathophysiology of LGE

Table 11 shows univariate analysis of the variables related to LGE. The presence of LGE was significantly associated with the finding of myocardial inflammation in biopsy (as detected by immunohistochemistry), with an ongoing myocyte necrosis (represented by increased hs-cTnT concentrations) and with a more advanced heart failure (as reflected by higher NYHA functional class and higher BNP concentrations).

In multivariate regression analysis only the biopsy finding of myocardial inflammation and BNP concentrations remained independent predictors of LGE (odds ratio [95 % CI] = 11.0 [1.3 - 96] and 3.5 [1.3 – 9.8] per ln ng/L; P = 0.03 and 0.017, respectively). BNP and NYHA class were included into the models separately because of a significant mutual correlation. In addition, the relative extent of LGE correlated with the hs-cTnT and BNP concentrations (r = 0.68 and 0.53, respectively; $P < 0.001$).

Interestingly, the extent of fibrosis evaluated in the biopsy specimens did not differ between the patients with and without LGE.

Table 11: Variables associated with occurrence of LGE in the left ventricle.

Variable	LGE absent n = 14	LGE present n = 28	p Value
NYHA class	2.2 ± 0.7	3.0 ± 0.8	0.006*
LV ejection fraction (%)	23 ± 11	21 ± 9	0.44
LV enddiastolic volume (ml/m^2)	128 ± 38	147 ± 42	0.19
LV enddiastolic diameter (mm)	67 ± 9	69 ± 7	0.47
LV mass (g/m^2)	108 ± 28	123 ± 23	0.59
B-type natriuretic peptide (ng/L)	283 [113–812]	1031 [592–1469]	0.003*
Hs-TnT (ng/L)	6 [4–16]	18 [9–54]	0.021*
Hs-TnT > 13.5 ng/L	4 (28 %)	19 (68 %)	0.02*
Troponin I > 0.03 µg/L	3 (21 %)	10 (36 %)	0.35
Troponin I maximum (µg/L)	0.3	3.6	—
GFR (ml/min/m^2)	74 ± 24	82 ± 18	0.40
Inflammation in EMB	2 (14 %)	13 (46 %)	0.04*
Fibrosis extent in EMB (%)	12 ± 5	16 ± 9	0.18

* The symbol highlights a p-value <0.05.

Figure 11: Variables associated with presence of LGE in new-onset DCM

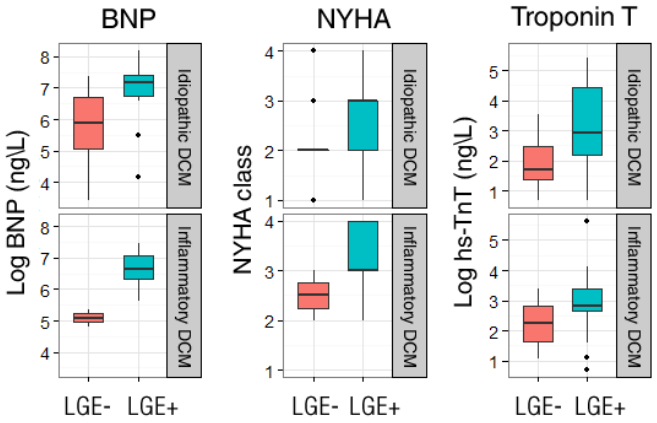

4.8 Occurrence of LVRR and its relation to clinical, exercise, echocardiographic and laboratory variables

A complete follow-up for evaluation of LVRR was available in 39 patients (89 %) that did not receive a heart transplant or a ventricular assist device. At 12 months, LVRR was observed in 20 individuals (45 %). But only 3 of the patients (7 %) improved LV ejection fraction above 50 %.

Tables 12–14 present comparison of variables recorded at baseline and at 3, 6 and 12 months with regard to LVRR at 12 months. Already after three months the patients with future LVRR had significantly smaller indexed LV enddiastolic diameter, improved LV diastolic function, decreased BNP, less frequent moderate or severe mitral regurgitation, smaller left atrial diameter and left atrial volume, lower resting heart rate, improved NYHA functional class and also improved all measures of functional exercise testing. Of note, at three months the LV and the RV ejection fraction did not yet differ from the patients without LVRR.

After 6 months, the patients with future LVRR differed even more significantly in the indexed LV enddiastolic diameter, LV diastolic function, levels of BNP, prevalence of mitral regurgitation and in the left atrial diameter and volume. In addition, at 6 months the patients with future LVRR had already significantly higher LV ejection fraction (but not RV ejection fraction) and smaller absolute LV enddiastolic diameter. After one year, the LVRR was accompanied—besides the default improvement of LV function and dimensions—by markedly improved functional capacity, absence of moderate or severe mitral regurgitation, a shorter QRS complex duration, lower BNP levels and also by improvement of RV ejection fraction (but not RV enddiastolic volume), as assed by CMR.

Table 12: Comparison of baseline variables with regard to LVRR—part I

Variable	Baseline data		Data at 1 year	
	LVRR− n = 24	LVRR+ n = 20	LVRR− n = 19	LVRR+ n = 20
Clinical variables				
Age	42 ± 14	45 ± 8	–	–
Males	16 (66 %)	15 (75 %)	–	–
Familiy history of DCM	8 (33 %)	3 (15 %)	–	–
Diabetes mellitus	1 (2 %)	1 (2 %)	–	–
Systemic hypertension	1 (4 %)	2 (10 %)	–	–
Viral prodroms	6 (25 %)	6 (30 %)	–	–
Duration of HF (months)	1.6 [1.0–4.0]	2.0 [1.0–3.0]	–	–
Decompensated HF	11 (46 %)	3 (15 %)*	–	–
NYHA I	1 (4 %)	0	2 (11 %)	14 (70 %)***
II	9 (37 %)	14 (70 %)	12 (63 %)	6 (30 %)
III	10 (42 %)	4 (20 %)	5 (26 %)	0
IV	4 (17 %)	2 (10 %)	0	0
BMI (kg/m^2)	25 ± 4	25 ± 3	27 ± 5	26 ± 4
Systolic BP (mm Hg)	111 ± 14	114 ± 20	112 ± 12	114 ± 17
Heart rate at rest (bpm)	85 ± 19	83 ± 19	73 ± 13	67 ± 9
Sinus rhythm (%)	24 (100 %)	19 (95 %)	19 (100 %)	20 (100 %)
QRS duration (ms)	108 ± 22	102 ± 21	114 ± 24	99 ± 16*
Left bundle-branch block	3 (12 %)	2 (10 %)	3 (16 %)	1 (5 %)
Exercise capacity				
Peak systolic BP (mm Hg)	130 ± 24	140 ± 18	138 ± 24	155 ± 18*
Peak heart rate (bpm)	138 ± 19	146 ± 13	132 ± 22	135 ± 18
VO_2 peak (ml/kg/min)	18.2 ± 6.2	20.6 ± 2.8	19.3 ± 6.8	23.1 ± 5.2*
VO_2 peak (% of predicted)	54 ± 20	60 ± 8	58 ± 20	69 ± 16*
VE/VCO_2 slope	31.0 ± 10.9	26.4 ± 6.6	29.4 ± 7.7	24.4 ± 3.7**
Biomarker testing				
Sodium (mmol/L)	140 ± 2	142 ± 2*	140 ± 2	141 ± 3
Creatinine (umol/L)	88 ± 19	104 ± 27*	80 ± 16	92 ± 27
GFR (ml/min)	86 ± 25	71 ± 18*	92 ± 25	84 ± 27
BNP (ng/L)	787 [376–1264]	375 [229–933]	172 [56–377]	25 [13–55]**
Hs-cTNT (ng/L)	17.5 [7.0–76.7]	9.5 [3.2–18.5]*	–	–
Hs-cTNT > 13.5 ng/L	15 (62 %)	8 (40 %)	–	–
Troponin I > 0.03 µg/L	9 (37 %)	4 (20 %)	–	–
Galectin-3 (µg/L)	3.6 [0.4–5.1]	1.5 [0.2–4.5]	–	–
Pharmacotherapy				
ACEI/ARB	21 (87 %)	19 (95 %)	16 (84 %)	19 (95 %)
ACEI/ARB ≥ 50 %	5 (21 %)	5 (25 %)	10 (53 %)	12 (60 %)
Beta-blockers	21 (87 %)	20 (100 %)	20 (100 %)	19 (100 %)
Beta-blockers ≥ 50 % of r.d.	6 (25 %)	5 (25 %)	18 (95 %)	16 (80 %)
Furosemide	22 (92 %)	18 (90 %)	15 (79 %)	13 (65 %)
Furosemide ≥ 40 mg/d	16 (67 %)	14 (70 %)	11 (58 %)	8 (40 %)
Intravenous diuretics	10 (42 %)	3 (15 %)	0	0
Spironolactone	21 (87 %)	14 (70 %)	14 (74 %)	9 (45 %)
Inotropes	5 (21 %)	1 (5 %)	0	0

*, **, *** denotes $p<0.05$, $p<0.01$, $p<0.001$; BP = blood pressure; HF = heart failure.

Table 13: Comparison of baseline variables with regard to LVRR—part II

Variable	Baseline data		Data at 1 year	
	LVRR− n = 24	LVRR+ n = 20	LVRR− n = 19	LVRR+ n = 20
Echocardiography				
LVEDD (mm)	69 ± 6	69 ± 7	67 ± 7	$58 \pm 5^{**}$
LVEDD indexed (mm/m)	40 ± 3	38 ± 3	39 ± 4	$33 \pm 2^{***}$
LV septum thickness (mm)	9 ± 1	9 ± 2	9 ± 1	9 ± 1
LV ejection fraction (%)	24 ± 8	22 ± 6	26 ± 6	$42 \pm 6^{***}$
Restrictive LV filling pattern	11 (46 %)	6 (30 %)	2 (11 %)	0
E/E' ratio	13.7 ± 5.5	12.5 ± 5.2	12.0 ± 3.6	$8.2 \pm 2.8^{**}$
LA diameter (mm/m)	27 ± 3	26 ± 4	25 ± 3	$21 \pm 3^{**}$
LA volume index (ml/m^2)	54 ± 21	43 ± 16	43 ± 16	$30 \pm 7^{**}$
MR grade ≥3 of 4	16 (67 %)	9 (42 %)	10 (53 %)	0^{***}
RVEDD (mm)	29 ± 6	29 ± 6	25 ± 4	26 ± 3
TAPSE (mm)	17 ± 4	18 ± 5	21 ± 3	22 ± 4
CMR				
LVEDV (ml/m^2)	147 ± 45	132 ± 35	113 ± 26	$71 \pm 12^{***}$
LV ejection fraction (%)	22 ± 10	21 ± 10	28 ± 5	$42 \pm 5^{***}$
LV mass (g/m^2)	106 ± 26	105 ± 28	86 ± 14	80 ± 18
RVEDV (ml/m^2)	80 ± 33	75 ± 27	66 ± 22	60 ± 13
RV ejection fraction (%)	23 ± 9	24 ± 8	35 ± 8	$45 \pm 7^{**}$
LGE present	18 (75 %)	12 (60 %)	7 (58 %)	8 (44 %)
LGE extent (g)	9.4 [2.4–16.4]	2.9 [0–8.4]*	4.6 [0–10.3]	0 [0–4.1]
Indexed LGE extent (%)	4.3 [1.1–7.8]	1.4 [0–4.3]**	2.2 [0–7.3]	0 [0–2.5]
Myocardial edema ratio	1.4 ± 0.2	$1.6 \pm 0.4^{*}$	1.2 ± 0.3	1.3 ± 0.2
Myocardial edema ratio > 1.9	0	4 (20 %)*	0	0
Early enhancement (%)	25.5 [17.9–42]	15.6 [6.6–36.9]	–	–
Early enhancement > 45 %	4 (18 %)	3 (15 %)	–	–
Biopsy findings				
Myocardial inflammation	5 (21 %)	10 (50 %)*	–	–
Virus positive (%)	17 (71 %)	12 (60 %)	–	–
Parvovirus B19 positive	17 (71 %)	10 (50 %)	–	–
Parvovirus B19 (copies/µg)	120 [0–547]	72 [0–922]	–	–
Other viruses	1 (4 %)	4 (20 %)	–	–
Extent of fibrosis	15.4 ± 8.2	13.5 ± 6.9	–	–

*, **, *** denotes p<0.05, p<0.01 and p<0.001, respectively

Table 14: Association between variables recorded at 3 and 6 months of follow-up and LVRR at 1 year of follow-up.

Variable	Data at 3 months		Data at 6 months	
	LVRR− n = 20	LVRR+ n = 20	LVRR− n = 19	LVRR+ n = 20
NYHA I	2 (10 %)	6 (30 %)**	3 (16 %)	9 (45 %)**
II	11 (55 %)	14 (70 %)	9 (47 %)	11 (55 %)
III	17 (35 %)	0	7 (37 %)	0
IV	0	0	0	0
ACEI/ARB	17 (85 %)	19 (95 %)	16 (84 %)	19 (95 %)
ACEI/ARB ≥ 50 % of r.d.	7 (35 %)	7 (35 %)	6 (32 %)	9 (45 %)
Beta-blockers	20 (100 %)	20 (100 %)	20 (100 %)	19 (100 %)
Beta-blockers ≥ 50 % of r.d.	10 (50 %)	9 (45 %)	14 (74 %)	13 (65 %)
Furosemide	16 (80 %)	18 (90 %)	15 (79 %)	16 (80 %)
Spironolactone	15 (75 %)	15 (75 %)	14 (74 %)	10 (50 %)
Furosemide ≥ 40 mg/d	12 (60 %)	15 (75 %)	12 (63 %)	11 (55 %)
Body mass index (kg/m^2)	26 ± 5	26 ± 3	27 ± 4	26 ± 4
Systolic BP at rest (mmHg)	110 ± 14	112 ± 11	114 ± 10	112 ± 12
Systolic BP peak† (mmHg)	129 ± 21	150 ± 19**	133 ± 19	152 ± 20**
Heart rate at rest (bpm)	82 ± 14	72 ± 11*	74 ± 15	70 ± 12
Heart rate peak† (bpm)	133 ± 19	145 ± 18	133 ± 22	136 ± 19
Sinus rhythm	20 (100 %)	19 (95 %)	19 (100 %)	20 (100 %)
QRS duration (ms)	110 ± 24	99 ± 17	110 ± 20	99 ± 16
Left bundle-branch block	3 (15 %)	1 (5 %)	3 (16 %)	1 (5 %)
LVEDD (mm)	69 ± 8	64 ± 8	67 ± 9	61 ± 6**
LVEDD indexed (mm/m)	40 ± 4	36 ± 4**	39 ± 4	34 ± 3***
LV septum thickness (mm)	9 ± 1	9 ± 2	9 ± 1	8 ± 1
LV ejection fraction (%)	26 ± 7	30 ± 7	28 ± 7	37 ± 10**
Restrictive LV filling	8 (40 %)	0**	2 (10 %)	0
E/E' ratio	13.4 ± 7.4	8.8 ± 3.3*	12.2 ± 3.7	8.0 ± 2**
LA diameter (mm/m)	25 ± 3	22 ± 3**	26 ± 4	21 ± 3***
LA volume index (ml/m^2)	46 ± 17	34 ± 10*	45 ± 17	30 ± 8**
Mitral regurgitation ≥3 of 4	10 (50 %)	3 (15 %)*	8 (42 %)	1(5 %)**
RVEDD (mm)	27 ± 4	27 ± 3	27 ± 3	27 ± 3
TAPSE (mm)	19 ± 4	21 ± 5	21 ± 4	20 ± 4
VO_2 peak† (ml/kg/min)	17.9 ± 5.5	22.2 ± 4.5**	18.0 ± 5.3	21.9 ± 3.2**
VO_2 peak† (% of predicted)	53 ± 19	65 ± 14**	54 ± 17	67 ± 14**
VE/VCO_2 slope†	30.1 ± 8.7	23.5 ± 3.2**	29.5 ± 8.8	24.5 ± 4.0**
Sodium (mmol/L)	141 ± 2	140 ± 2	140 ± 2	140 ± 2
Creatinine (umol/L)	85 ± 27	91 ± 26	79 ± 16	94 ± 25*
GFR (ml/min)	91 ± 29	84 ± 24	94 ± 28	81 ± 25
BNP (ng/L)	350 [149–731]	101 [70–196]**	244 [66–538]	53 [36–70]***

*, **, *** denotes p<0.05, p<0.01, p<0.001; † corresponds to data obtained during exercise testing; BP = blood pressure.

4.8.1 CMR findings after 12 months of follow-up

A follow-up CMR was available in 30 non-transplanted individuals that did not have implanted a metallic cardiac device. At baseline, LGE was present in 20 of 30 patients (67 %) with the follow-up CMR. At 12 months, LGE persisted in 13 (43 %) and disappeared in another 7 (23 %). Out of 10 patients who did not present with LGE at baseline, 8 (27 %) remained without LGE but (7 %) developed a new LGE lesion. Pattern and localization of the LGE in the LV did not differ with respect to the LVRR. Importantly, both the LGE extent and the myocardial edema ratio decreased during the follow-up (5.5 [0-12] vs. 1.3 [0-6] g, P = 0.001; and 1.53 ± 0.37 vs. 1.29 ± 0.25, P = 0.002; respectively). A typical finding of a reduced LGE at the 12-months examination is presented in Figure 12. The baseline values of the LGE extent and the myocardial edema ratio significantly differed between the patients without and with LVRR (Table 13). On the other hand, the absolute or relative changes in the LGE extent and myocardial edema ratio did not differ with respect to the LVRR (absolute [relative] change; no LVRR vs. LVRR; LGE extent, -2.7 ± 4.8 vs. -3.9 ± 5.0 % [-60 ± 48 vs. -46 ± 40 %], P = 0.46; myocardial edema ratio; -0.17 ± 0.25 vs. -0.33 ± -0.48 [-110 ± 18 vs. 116 ± 22 %], P = 0.32).

4.9 Prediction of LVRR from baseline data

In the univariate analysis, 9 of 70 baseline variables predicted the subsequent LVRR (Table 12). Compared with the remaining individuals, LVRR was heralded by lower serum levels of hs-cTNT, higher plasma levels of sodium and, surprisingly, by worse renal function. Other predictive parameters included a higher prevalence of myocardial inflammation in biopsy and two CMR variables—a smaller extent of LGE and a higher myocardial edema ratio.

Neither the presence of viral genomes nor the extent of fibrosis in EMB samples were related to LVRR. A multivariate analysis identified only two independent predictors of LVRR at baseline: a lower value of the indexed LGE extent and a higher value of the myocardial edema ratio (Table 16). A simultaneous positivity of both variables predicted LVRR with a sensitivity of 70 % and a specificity of 78 % (Table 15).

4.10 Prediction of LVRR from the follow-up data

In the univariate analysis, 15 of 60 follow-up variables predicted LVRR. These predictors included a better exercise capacity, a lower LVEDD, a higher LV ejection

fraction, less severe mitral regurgitation, a smaller left atrial volume and lower values of non-invasive indicators of the LV filling pressure (E/E' ratio, presence of restrive mitral pattern, BNP plasma level) (Figure 13 and Table 14). Importantly, there were no differences in the use of heart failure medication in both groups. At 3 months, the latest plasma level of BNP was the only independent predictor of LVRR (Table 16). Specifically, BNP level < 344 ng/L predicted LVRR with a sensitivity of 95 % and a specificity of 50 % (Table 15). The conventional methods (LVEDD index and E/E' ratio) became independent predictors of LVRR as late as after 6 months of follow-up. Both the baseline indexed LGE extent and the myocardial edema ratio remained independent predictors of LVRR when combined with the BNP plasma level at 3 months or with the LVEDD index and the E/E' ratio at 6 months (Table 16).

Figure 12: Change in the extent of LGE after 1 year with regard to LVRR

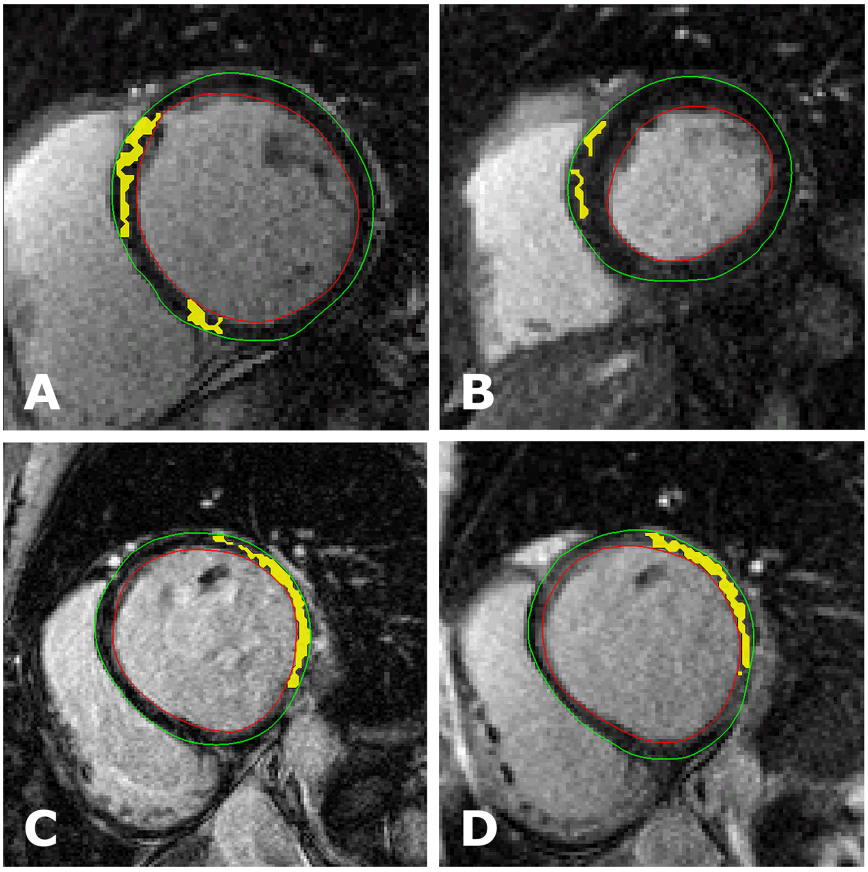

The yellow areas indicate a signal intensity >2 standard deviations above the mean of the remote reference myocardium. Panels A and B demonstrate corresponding short-axis slices at baseline and 12 months follow-up in a patient with LVRR. Panels C and D show similar images in a patient without LVRR. There was a marked reduction in the extent of LGE in the patient with LVRR but there was virtually no change in the extent of LGE in the patient without LVRR.

Figure 13: Longitudinal changes in LVEDD and median BNP levels in patients with and without LVRR

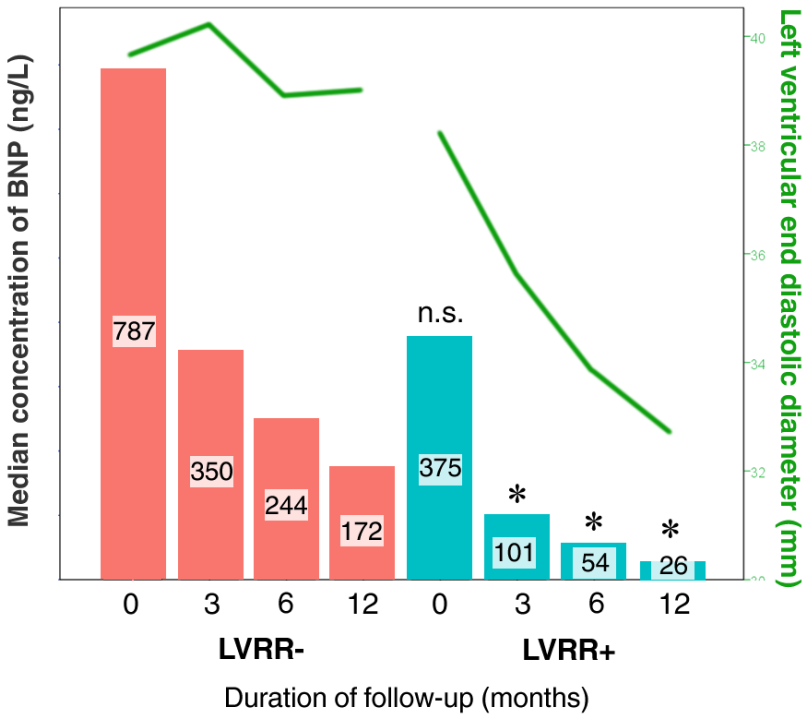

Table 15: Results of receiver operator characteristics analysis with selected cut-off points of variables predicting left ventricular reverse remodeling.

	Variable	Cut-off	SN	SP	AUC [95% CI]	P
BL	Indexed LGE extent (%)	< 5	90	46	0.73 [0.58–0.88]	0.009
	Edema ratio	≥1.30	80	44	0.67 [0.51–0.84]	0.043
	Indexed LGE extent + edema ratio	<5 and ≥1.30	70	78		
3 M	BNP (ng/L)	<344	95	50	0.79 [0.64–0.94]	0.002
6 M	LVEDD (mm/m)	<38	85	68	0.83 [0.70–0.96]	0.000
	E/E' ratio	<11.7	100	53	0.82 [0.69–0.96]	0.001
	BNP (ng/L)	<168	95	63	0.81 [0.67–0.95]	0.001
	LVEDD and E/E' ratio	<38 and <11.7	85	84		
	LVEDD and BNP	<38 and <168	80	79		

BL, 3 M and 6 M = baseline, 3 months and 6 months; AUC = area under the curve; CI = confidence interval; P = p-Value; SN = sensitivity; SP = specificity.

Table 16: Results of multivariate analysis showing independent predictors of LVRR at baseline, 3 and 6 months of follow-up.

Multivariate model	Odds ratio [95% CI]	p Value
(1) Baseline		
Indexed LGE extent†	0.67 [0.50–0.90]	0.008**
Myocardial edema ratio‡	1.45 [1.04–2.02]	0.027*
(2) 3 months		
B-type natriuretic peptide§	0.14 [0.02–0.94]	0.042*
(3) 6 months		
LVEDD index¶	0.73 [0.56–0.96]	0.014*
E/E' ratio	0.56 [0.33–0.94]	0.019*
(4) Baseline + 3 months		
B-type natriuretic peptide at 3 months§	0.13 [0.01;0.96]	0.001**
Myocardial edema ratio at baseline‡	1.37 [1.18–1.93]	0.048*
Indexed LGE extent at baseline†	0.75 [0.55–0.93]	0.028*
(5) Baseline + 3 months + 6 months		
E/E' ratio at 6 months	0.45 [0.20–0.98]	<0.001***
LVEDD index at 6 months¶	0.78 [0.59–0.95]	0.005**
Indexed LGE extent at baseline†	0.69 [0.45–0.96]	0.047*
Myocardial edema ratio at baseline‡	1.57 [1.12–2.7]	0.027*

† signifies odds ratio per % of LV mass; ‡, per 0.1 unit; §, per log(µg/l); ¶, per mm/m, respectively.

Variables which were entered in the multivariate analysis:

Model 1 (baseline data): decompensated heart failure at admission, sodium plasma level, estimated glomerular filtration rate, high-sensitivity cardiac troponin T, LGE extent, myocardial edema ratio, presence of myocardial inflammation in biopsy

Model 2 (3-month data) : NYHA functional class, heart rate, LVEDD index, restrictive mitral pattern, severity of mitral regurgitation, left atrial volume index, peak exercise systolic blood pressure, peak oxygen consumption, VE/VCO2 slope, Log BNP.

Model 3 (6-month data): NYHA functional class, LVEDD index, LV ejection fraction, E/Em, left atrial volume index, peak exercise systolic blood pressure, peak oxygen consumption, VE/VCO2 slope, Log BNP.

Model 4 (independent predictors from model 1 and 2): indexed LGE extent, myocardial edema ratio, Log BNP (3 months).

Model 5 (independent predictors from models 1 to 3): indexed LGE extent, myocardial edema ratio, Log BNP (3 months), LVEDD index (6 months), E/Em (6 months).

4.11 Prediction of adverse clinical events

Besides evaluation of LVRR at 12 months of follow-up, the patients were followed for 25 ± 9 months for occurrence of adverse clinical events. During this period, 8 patients (18 %) were readmitted for decompensation of heart failure, 4 (9 %) received a ventricular assist device, 4 (9 %) underwent an urgent heart transplantation and another 4 (9 %) died. The causes of the deaths included rapid progression of multiorgan failure (n=1), sudden cardiac death (n=1) and fatal complications related to the implantation of the ventricular assist device (n=2).

Twelve patients (27 %) reached a composite clinical end point which was defined by occurrence of any of the above events, order by their severity: cardiac death (n = 4), urgent heart transplantation (n = 4) and hospitalization for decompensation of heart failure (n = 4). Two of the transplanted patients and two of the deceased patients had implanted a ventricular assist device. By univariate analysis, the composite clinical endpoint was associated with a higher NYHA class, increased BNP levels, presence of LGE, greater extent of LGE and increased baseline concentrations of hs-cTnT.

The time of the occurrence of the events, with regard to the baseline presence of LGE is depicted on the Kaplan-Meier plot on the Figure 14. In Cox's multivariate regression models only the increased hs-cTnT concentration remained an independent predictor of the end point.

Unfortunately, the study was underpowered to identify any predictors of a composite "hard" clinical endpoint consisting of mortality, urgent heart transplantation or implantation of mechanical ventricular assist device, not considering the hospitalization for heart failure. An implantable cardioverter-defibrillator for primary prevention of sudden arrhythmic death was implanted in 12 (27 %) patients. Only one of them had an adequate shock for ventricular fibrillation at 1.5 years of follow-up. Additional 4 patients with left bundle-branch block received a biventricular pacemaker for resynchronization therapy (at 12, 14, 19 and 21 months of follow-up).

Table 17: Univariate analysis of the variables associated with the composite end point of cardiac death, urgent heart transplanation, or hospitalization for worsening of heart failure.

Variable	HR [95% CI]	p Value
Male	1.3 [0.4–4.3]	0.72
Age (per year)	0.96 [0.9–1.0]	0.14
Serum creatinine (per mg/dL)	0.99 [0.9–1.0]	0.49
NYHA class	2.2 [1.1–4.8]	0.028*
B-type natriuretic peptide (per log(ng/L))	2.7 [1.2–6.2]	0.022*
High-sensitivity troponin T (per log(ng/L))	2.2 [1.4–3.5]	0.001**
High-sensitivity troponin T > 13.5 pg/L	5.1 [1.1–23]	0.035*
Idexed LGE extent (per % of LV mass)	1.1 [1.0–1.2]	0.008**
LGE present	6.3 [0.8–49]	0.044*
Edema ratio (per unit)	0.5 [0.1–3.6]	0.46
Early gadolinium enhancement (per %)	1.0 [1.0–1.0]	0.33
Pericardial effusion (per ml)	2.5 [0.8–8.2]	0.13
Myocardial inflammation in biopsy	1.3 [0.4–4.2]	0.64
Viral genoma in biopsy	1.6 [0.5–5.0]	0.44
Extent of fibrosis in biopsy (per %)	1.0 [0.9–1.1)	0.27

HR = hazard ratio; CI = confidence interval.

Table 18: Univariate and multivariate predictors of the composite end point of cardiac death, urgent heart transplanation, or hospitalization for worsening of heart failure.

Variables	Univariate analysis		Cox's regression models	
	HR [95% CI]	p Value	HR (95% CI)	p Value
Gender (male)	1.3 [0.4–4.3]	0.72		
Age (years)	0.96 [0.9–1.0]	0.14		
Creatinine (mg/dL)	0.99 [0.9–1.0]	0.49		
NYHA class	2.2 [1.1–4.8]	0.028*		
BNP (per log(ng L))	2.7 [1.2–6.2]	0.022*	8.3 [0.7–97.2]	0.09
Hs-TnT (per log(ng L))	2.2 [1.4–3.5]	0.001**	5.3 [1.3–21.3]	0.019*
Inflammation in EMB	1.3 [0.4–4.2]	0.64		
Extent of fibrosis in EMB (%)	1.0 [0.9–1.1]	0.27		
Extent of LGE (% of LV mass)	1.1 [1.0–1.2]	0.008**	3.1 (0.9–11.0)	0.066

HR = hazard ratio; CI = confidence interval.

Figure 14: Kaplan-Meier analysis of a mid-term freedom from a composite endpoint of adverse clinical events according to the baseline presence of LGE

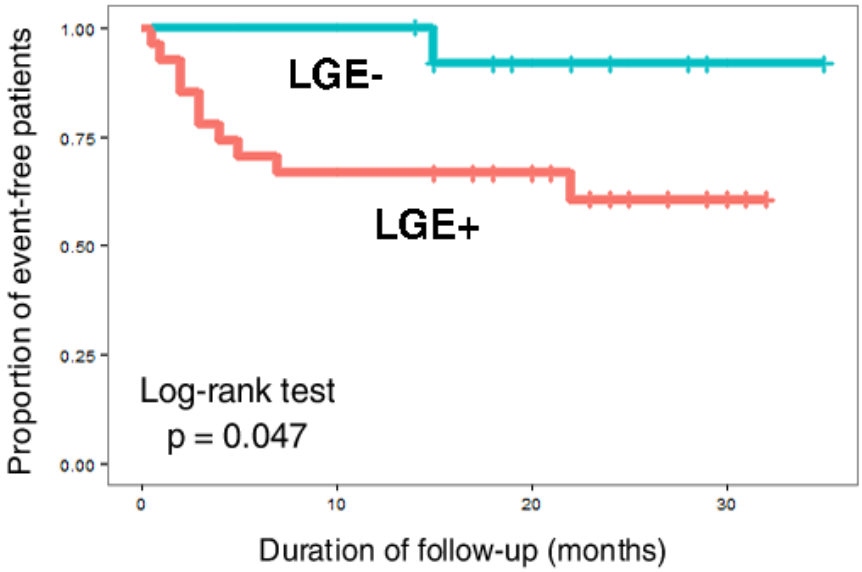

The figure shows Kaplan-Meier freedom from a composite endpoint of death related to heart failure, urgent heart transplantation and readmission for worsening of heart failure, using the baseline presence of LGE as the strata. LGE-/+ signifies absence/presence of LGE at the baseline examination.

5 Discussion

5.1 The main contribution of this work

This is the first study that systematically evaluated use of a novel multisequential CMR protocol for assessment of pathophysiological processes in the individuals with new-onset DCM. In addition, our study was able to demonstrate prognostic value of the pathological CMR findings with regard to LVRR. One of the main strengths of the study was the complexity of the collected data: besides the CMR scans, we had available histopathological and immunohistochemical assessment of the myocardial tissue; biomarker data reflecting hemodynamic status and activity of myocardial necrosis; a thorough clinical assessment which included functional exercise testing; and a rigorous mid-term clinical follow-up. At last, serial CMR scans enabled to intercept evolution of the myocardial pathological processes and its relationship to the LVRR.

5.2 Major findings

Among the extensive data obtained in the study there are several findings that should be highlighted:

1. Myocardial inflammation was a common finding in the individuals with new-onset DCM, though the inflammation had generally a low activity.
2. The overall performance of CMR for detection of myocardial inflammation was rather modest. LGE was a sensitive sign for myocardial inflammation, however it was also a hallmark of more advanced heart failure. Myocardial early enhancement and pericardial effusion were specific but uncommon findings. Imaging of myocardial edema by T2-weighted imaging was not useful for the diagnosis.
3. The concurrent use of CMR, EMB and novel cardiac biomarkers provided new insights into pathophysiology of LGE in new-onset DCM. In particular, we demonstrated that in new-onset DCM the presence of LGE may be equally attributed to myocardial inflammation and to an ongoing myocardial necrosis damage due to the LV hemodynamic overload. Importantly, in some patients the LGE had receded or even disappeared over one year and this receding of the LGE was paralleled with the LVRR.
4. A lower extent of LGE and a higher myocardial edema ratio were independent baseline predictors of LVRR at 12 months. In fact, at baseline these

CMR markers outperformed BNP, EMB and conventional methods for prediction of LVRR. Although at a later stage of the disease the actual BNP levels, LVEDD and E/E' ratio became the strongest predictors of the LVRR, the baseline LGE and the myocardial edema ratio retained their independent predictive value. In addition, the presence of LGE was also a strong predictor of future adverse clinical events, such as cardiac death, urgent heart transplantation and rehospitalization for heart failure.

5.3 CMR for detection of myocardial inflammation

The value of CMR for detection of clinically suspected acute myocarditis has been repeatedly demonstrated (Friedrich et al. 2009). But, similar data are lacking for the patients with new-onset DCM who have no clinical signs of myocarditis. Recently, Voigt and colleagues evaluated the diagnostic performance of CMR for detection of immunohistologically confirmed myocardial inflammation in 23 DCM patients with a history of heart failure longer than 3 months (Voigt et al. 2011). They reported the overall sensitivity, specificity and diagnostic accuracy of CMR of 75 %, 73 % and 74 %, respectively. These results are similar to the overall sensitivity, specificity and accuracy of 67 % , 85 % and 79 % found in our study.

In contrast to the study by Voigt and several other studies in patients with acute myocarditis, we found that the T2-weighted imaging did not add any diagnostic value to the CMR protocol. Moreover, we found rather a modest diagnostic value of the myocardial early enhancement technique. The limited performance of the two CMR techniques found by our study could be explained by the fact that the target pathophysiological processes (myocardial edema, hyperperfusion and capillary leakage) were less expressed in our patients than in an acute myocardial inflammation (De Cobelli et al. 2006, Friedrich et al. 1998).

Gutberlet and colleagues observed LGE only in 24 % of patients with clinically suspected "borderline" myocarditis and preserved LV dysfunction (Gutberlet et al. 2008). The LGE had 80 % specificity for myocarditis. In contrast, the LGE was present in 67 % of our patients (who had also mostly low-activity myocarditis but with severe LV dysfunction), though the finding had only 44 % specificity for myocarditis. The higher prevalence of LGE found in the patients with LV dysfunction and the lower specificity of this finding for myocarditis could be explained by the fact that the LGE in DCM may also reflect pathophysiological processes that are related to the heart failure itself. In this regard, the increased levels of BNP and cardiac troponin in our patients with LGE support a previously proposed hypothesis that an increased wall stress in the overloaded dilated LV may lead to relative myocardial ischemia, which in turn may result to myocyte necrosis (Alter et al.

2007). In fact, by combining the results of CMR, EMB and cardiac biomarkers we were able to show that the LGE in the patients with new-onset DCM accounts roughly by an equal part for myocardial inflammation and by an equal part for the hemodynamic stress. Furthermore, in DCM patients the LGE seem to be more common in an earlier stage of the disease (56 % in the study by Voigt and 67 % in our study) than at a chronic stage (39–41 % Lehrke et al. (2011), Wu et al. (2008)). This could be explained by a natural or pharmacotherapy-induced resolution of either the myocarditis or by the resolution of the stress-related myocardial injury. Finally, the myocardial injury, regardless of the etiology, can recede or eventually it can heal with a fibrotic scar. The scar may then appear as LGE. Thus, the pathophysiology of LGE in DCM must be interpreted in the context of the disease duration and the hemodynamic status.

5.4 CMR for predicting LVRR and clinical outcome in new-onset DCM

The concept of LVRR was introduced by Dec & Fuster (1994). A larger study by Steimle et al. (1994), conducted before the era of beta-blockers, observed LVRR in 27 % of patients with DCM. Over time, advances in heart failure pharmacotherapy have increased the incidence of LVRR in general heart failure population (Binkley et al. 2012, Wilcox et al. 2012) and also in the subpopulation of new-onset DCM (McNamara et al. 2011). In the Intervention in Myocarditis and Acute Cardiomyopathy trials IMAC-1 and IMAC-2 the incidence of LVRR reached 56 % at 12 months and 70 % at 6 months, respectively (McNamara et al. 2001, 2011). In agreement with the IMAC-1 study we observed LVRR in 45 % patients.

In the study by Steimle the LVRR was associated with a shorter symptom duration and less severe hemodynamic decompensation (Steimle et al. 1994). Interestingly, the finding of myocarditis in EMB (using the Dallas criteria) did not predict the LVRR. In line with Steimle, in univariate analysis we found significant association between biopsy-confirmed myocardial inflammation and LVRR but the predictive value of this finding was not confirmed in the multivariate models. In the IMAC-2 trial, the LVRR was associated with a lower NYHA functional class, lower LVEDD and a higher systolic blood pressure. However, none of the variables were robust enough to aid the clinical decision making (McNamara et al. 2011).

In our study we introduced novel predictors of LVRR that are much more robust than those previously reported, in particular the variables derived from CMR and serial BNP testing. In addition, we evaluated the predictors of LVRR not only at baseline but also longitudinally. As a result, we could identify specific cut-off

points for each follow-up period and showed that the novel predictors provided an earlier prediction of LVRR than the conventional methods.

Previously, the prognostic value of CMR was investigated mostly in the patients with long-term established diagnosis of DCM (Assomull et al. 2006, Wu et al. 2008). The study by Leong and colleagues was the first to focus on the newly manifested DCM (Leong et al. 2012). The authors demonstrated strong negative correlation between the extent of LGE and improvement of LV systolic function. Unfortunately, the study was limited by the fact that the improvement in LV was defined by somewhat clinically irrelevant 5 % increase in the LV ejection fraction. Moreover, the study by Leong excluded all individuals with possible myocarditis (which was defined by abnormal troponin or evidence of myocardial edema on T2-weighted imaging), but tachycardia-induced cardiomyopathy was not considered to be an exclusion criterion.

In our study, we excluded only individuals with suspected tachycardia-induced cardiomyopathy and alcoholic cardiomyopathy because they are recognized as highly reversible disease entities. We found no good reason not to recruit troponin I positive individuals with new-onset DCM who represented almost one third of our consecutive patients. We believe that our inclusion criteria, the definition of LVRR and the structured one year follow-up better support the applicability of our results in the clinical practice.

Importantly, extent of myocardial damage, as assessed by CMR, not only predicts the LVRR but it is a robust predictor of mortality in inflammatory (Wilcox et al. 2012) as well as in idiopathic DCM (Steimle et al. 1994, Binkley et al. 2012). Our study expands the available evidence by confirming the prognostic role of LGE also in the patients with new-onset DCM. All these data justify the routine use of CMR in patients with newly diagnosed DCM.

5.5 Pathophysiology of LVRR

Despite the long-term recognition of the phenomenon of LVRR a little is known about the underlying pathophysiology, especially if the LVRR occurs spontaneously. Though the LVRR is primarily defined as a decrease in the LV volume and improvement of the contractile function, complex structural and functional changes have been described at the cellular and tissue level (Koitabashi & Kass 2012). For certain etiologies of DCM, the LVRR may occur once the triggering insult is resolved. Currently, there are three major etiologies of DCM that are associated with a high rate LVRR and even with full LV recovery. These include DCM caused by tachycardias (above all, by atrial fibrillation), by toxic insults and

by myocardial inflammation. The first two can be readily diagnosed by clinical presentation and medical history. The later can be detected by endomyocardial biopsy or less reliably by CMR. In addition, we have demonstrated by a repeated CMR, that the LVRR parallels resolution of the initial tissue pathology.

5.6 Therapeutic implications

Determining the etiology of DCM in an affected individual may be clinically relevant. The patients with inflammatory DCM seem to have somewhat better prognosis than the patients with idiopathic DCM, though our study was unable to confirm similar observations (Givertz & Mann 2013).

Furthermore, besides naturally more favorable course of the disease, the patients with inflammatory DCM may receive a specific therapy targeting inflammation on top of the standard management of heart failure. Improvement in LV ejection fraction by >15-20 % have been reported in several smaller case series using immunosuppression, immunoadsorption or anti-viral therapy (Kindermann et al. 2012). However, no study assessed mortality or morbidity benefits of such treatments in patients with DCM.

One of the reasons for the lack of larger studies on inflammation-targeted treatment in DCM is the difficulty to select appropriate candidates for the treatment. Screening for inflammatory DCM solely by EMB may be limited by its low diagnostic yield. In fact, Frustaci had to perform 500 biopsies to identify only 85 (17 %) potential candidates for immunosuppressive therapy (Frustaci et al. 2009). The proportion was even lower (3 %) in the study of Maisch et al. (2007). In this context, CMR may probably not fully replace EMB in establishing the diagnosis before initiation of a specific treatment; however, the LGE could serve as a selection criterion for referring patients with new-onset DCM for EMB. Of note, in our study group such approach would prevent many unnecessary biopsies with a high negative predictive value.

The role of CMR (specifically the extent of LGE) to predict response to pharmacotherapy in chronic heart failure patients was reported by Bello and colleagues already in 2003 (Bello et al. 2003). It was the first study that opened the door to the personalized medicine in this field. Improved prediction of clinical outcome among individuals with new-onset DCM might be helpful for the cost-effective use of implantable cardioverter-defibrillators in the primary prevention of sudden cardiac death and it could also be used for optimal timing of referral to heart transplantation. Therefore, we propose to include CMR into the routine baseline assessment of all patients with new-onset DCM.

5.7 Study limitations

The relatively small size of the study sample may have influenced the power of the statistical analysis. To prevent overfitting, the multivariate regression models were restricted to a maximum of 2 independent variables, because the total number of the followed events was <30 (Peduzzi et al. 1995). The main reason for the restricted study size was its complex design. Besides a thorough clinical and laboratory investigation, repeated CMR exams and a detailed clinical follow-up the patients underwent an invasive procedure - EMB.

The EMB was performed only from the right-ventricular side of the interventricular septum. This could have introduced a sampling bias. The diagnostic yield could have been improved by targeting the biopsy to the sites with a pathological finding on CMR or by harvesting the samples from the LV cavity (Mahrholdt et al. 2004). On the other hand, these alternative approaches of EMB could have jeopardized the patients' safety and they would have made the procedure substantially more complex. In fact, we have demonstrated that the prevalence of myocarditis detected by right ventricular approach was not dependent on the localization of the LGE in the LV. This finding implies that our EMB results might not have been significantly influenced by the chosen approach.

For evaluation of the patients' hemodynamic status we used BNP levels as a surrogate of the LV filling pressure. Although the biomarker is routinely used for this purpose in the clinical practice, an invasive measurement of the filling pressures would be more appropriate. On the other hand, this would require either right heart catheterization or an additional LV catheterization through an arterial approach, thus further increasing the risk of complications.

We used one of several previously proposed immunohistochemical arbitrary definitions of myocardial inflammation. Various other definitions have been used by other investigators. In fact, the lack of the standardization of the immunohistochemical criteria might cause a comparison between future studies problematic.

For evaluation of global early enhancement we used a method proposed by Laissy et al. (2002). We preferred this approach mainly because of an extensive experience with this technique in our institution. Although this technique has been validated against EMB, recently a consensus of experts suggested to use a slightly different, more specific, method for the evaluation of early enhancement.

We evaluated the presence and extent of LGE in the LV irrespective of its pattern and localization in the LV. In fact, various patterns a localization of the LV could have represented a different underlying pathology, which in turn could be related to a different clinical outcome. Nevertheless, we have demonstrated

that the presence of LGE per se is an independent marker of LVRR and adverse clinical events.

Finally, although the used definition of LVRR has been used by previous investigators, such definition is rather specific for patients with severe LV dysfunction. Different cut-offs might be suitable for different populations.

6 Conclusions

In patients with new-onset DCM, CMR has suboptimal accuracy for detection of myocardial inflammation mainly because the activity of the inflammation is generally low. On the other hand, CMR can be used for noninvasive evaluation of hemodynamic stress and extent of myocardial damage. LVRR is relatively common, but complete recovery of the left ventricular dysfunction is rare. The pathological CMR findings, specifically the extent of LGE and the myocardial edema ratio provide at a baseline examination a better prediction of the LVRR than endomyocardial biopsy, BNP and conventional methods of cardiologic follow-up.

References

Abdel-Aty, H., Boye, P., Zagrosek, A., Wassmuth, R., Kumar, A., Messroghli, D., Bock, P., Dietz, R., Friedrich, M. G. & Schulz-Menger, J. (2005), 'Diagnostic performance of cardiovascular magnetic resonance in patients with suspected acute myocarditis: comparison of different approaches.', *J Am Coll Cardiol* **45**(11), 1815–22.

Alter, P., Rupp, H., Rominger, M. B., Vollrath, A., Czerny, F., Klose, K. J. & Maisch, B. (2007), 'Relation of B-type natriuretic peptide to left ventricular wall stress as assessed by cardiac magnetic resonance imaging in patients with dilated cardiomyopathy.', *Can J Physiol Pharmacol* **85**(8), 790–9.

Ammann, P., Naegeli, B., Schuiki, E., Straumann, E., Frielingsdorf, J., Rickli, H., Bertel, O., Karjalainen, J. & Heikkila, J. (1986), 'Acute pericarditis: myocardial enzyme release as evidence for myocarditis.', *Int J Cardiol* **111**(3), 546–52.

Aretz, H. T., Billingham, M. E., Edwards, W. D., Factor, S. M., Fallon, J. T., Fenoglio, J. J., J., Olsen, E. G. & Schoen, F. J. (1987), 'Myocarditis. A histopathologic definition and classification.', *Am J Cardiovasc Pathol* **1**(1), 3–14.

Assomull, R. G., Prasad, S. K., Lyne, J., Smith, G., Burman, E. D., Khan, M., Sheppard, M. N., Poole-Wilson, P. A. & Pennell, D. J. (2006), 'Cardiovascular magnetic resonance, fibrosis, and prognosis in dilated cardiomyopathy.', *J Am Coll Cardiol* **48**(10), 1977–85.

Baldasseroni, S., Opasich, C., Gorini, M., Lucci, D., Marchionni, N., Marini, M., Campana, C., Perini, G., Deorsola, A., Masotti, G., Tavazzi, L. & Maggioni, A. P. (2002), 'Left bundle-branch block is associated with increased 1-year sudden and total mortality rate in 5517 outpatients with congestive heart failure: a report from the Italian network on congestive heart failure.', *Am Heart J* **143**(3), 398–405.

Bello, D., Shah, D. J., Farah, G. M., Di Luzio, S., Parker, M., Johnson, M. R., Cotts, W. G., Klocke, F. J., Bonow, R. O., Judd, R. M., Gheorghiade, M. & Kim, R. J. (2003), 'Gadolinium cardiovascular magnetic resonance predicts reversible myocardial dysfunction and remodeling in patients with heart failure undergoing beta-blocker therapy.', *Circulation* **108**(16), 1945–53.

Bello, D., Shah, D. J., Farah, G. M., Di Luzio, S., Parker, M., Johnson, M. R., Cotts, W. G., Klocke, F. J., Bonow, R. O., Judd, R. M., Gheorghiade, M., Kim, R. J., Merlo, M., Pyxaras, S. A., Pinamonti, B., Barbati, G., Di Lenarda, A. & Sinagra, G. (2011), 'Prevalence and prognostic significance of left ventricular reverse remodeling in dilated cardiomyopathy receiving tailored medical treatment.', *Circulation* **57**(13), 1468–76.

Binkley, P. F., Lesinski, A., Ferguson, J. P., Hatton, P. S., Yamokoski, L., Hardikar, S., Cooke, G. E., Leier, C. V., Wilcox, J. E., Fonarow, G. C., Yancy, C. W., Albert, N. M., Curtis, A. B., Heywood, J. T., Inge, P. J., McBride, M. L., Mehra, M. R., O'Connor, C. M., Reynolds, D., Walsh, M. N. & Gheorghiade, M. (2012), 'Factors associated with improvement in ejection fraction in clinical practice among patients

with heart failure: findings from IMPROVE HF.', *Am Heart J* **163**(1), 49–56.

Bogaert, J. & Francone, M. (2009), 'Cardiovascular magnetic resonance in pericardial diseases.', *J Cardiovasc Magn Reson* **11**, 14.

Caforio, A. L. & Iliceto, S. (2008), 'Genetically determined myocarditis: clinical presentation and immunological characteristics.', *Curr Opin Cardiol* **23**(3), 219–26.

Chow, L. H., Radio, S. J., Sears, T. D. & McManus, B. M. (1989), 'Insensitivity of right ventricular endomyocardial biopsy in the diagnosis of myocarditis.', *J Am Coll Cardiol* **14**(4), 915–20.

Cooper, L. T. (2009), 'Myocarditis.', *N Engl J Med* **360**(15), 1526–38.

Cooper, L. T., Baughman, K. L., Feldman, A. M., Frustaci, A., Jessup, M., Kuhl, U., Levine, G. N., Narula, J., Starling, R. C., Towbin, J. & Virmani, R. (2007), 'The role of endomyocardial biopsy in the management of cardiovascular disease: a scientific statement from the American Heart Association, the American College of Cardiology, and the European Society of Cardiology. Endorsed by the Heart Failure Society of America and the Heart Failure Association of the European Society of Cardiology.', *J Am Coll Cardiol* **50**(19), 1914–31.

De Cobelli, F., Pieroni, M., Esposito, A., Chimenti, C., Belloni, E., Mellone, R., Canu, T., Perseghin, G., Gaudio, C., Maseri, A., Frustaci, A. & Del Maschio, A. (2006), 'Delayed gadolinium-enhanced cardiac magnetic resonance in patients with chronic myocarditis presenting with heart failure or recurrent arrhythmias.', *J Am Coll Cardiol* **47**(8), 1649–54.

Dec, G. W. (2014), 'The natural history of acute dilated cardiomyopathy.', *Trans Am Clin Climatol Assoc* **125**, 76–87.

Dec, G. W. & Fuster, V. (1994), 'Idiopathic dilated cardiomyopathy.', *N Engl J Med* **331**(23), 1564–75.

Dickstein, K., Cohen-Solal, A., Filippatos, G., McMurray, J. J., Ponikowski, P., Poole-Wilson, P. A., Stromberg, A., van Veldhuisen, D. J., Atar, D., Hoes, A. W., Keren, A., Mebazaa, A., Nieminen, M., Priori, S. G. & Swedberg, K. (2008), 'ESC Guidelines for the diagnosis and treatment of acute and chronic heart failure 2008: the Task Force for the Diagnosis and Treatment of Acute and Chronic Heart Failure 2008 of the European Society of Cardiology. Developed in collaboration with the Heart Failure Association of the ESC (HFA) and endorsed by the European Society of Intensive Care Medicine (ESICM).'.

Elliott, P., Andersson, B., Arbustini, E., Bilinska, Z., Cecchi, F., Charron, P., Dubourg, O., Kuhl, U., Maisch, B., McKenna, W. J., Monserrat, L., Pankuweit, S., Rapezzi, C., Seferovic, P., Tavazzi, L. & Keren, A. (2008), 'Classification of the cardiomyopathies: a position statement from the European Society Of Cardiology Working Group on Myocardial and Pericardial Diseases.', *Eur Heart J* **29**(2), 270–6.

Feldman, A. M. & McNamara, D. (2000), 'Myocarditis.', *N Engl J Med* **343**(19), 1388–

98.

Friedrich, M. G., Sechtem, U., Schulz-Menger, J., Holmvang, G., Alakija, P., Cooper, L. T., White, J. A., Abdel-Aty, H., Gutberlet, M., Prasad, S., Aletras, A., Laissy, J. P., Paterson, I., Filipchuk, N. G., Kumar, A., Pauschinger, M. & Liu, P. (2009), 'Cardiovascular magnetic resonance in myocarditis: A JACC White Paper.', *J Am Coll Cardiol* **53**(17), 1475–87.

Friedrich, M. G., Strohm, O., Schulz-Menger, J., Marciniak, H., Luft, F. C. & Dietz, R. (1998), 'Contrast media-enhanced magnetic resonance imaging visualizes myocardial changes in the course of viral myocarditis.', *Circulation* **97**(18), 1802–9.

Frustaci, A., Russo, M. A. & Chimenti, C. (2009), 'Randomized study on the efficacy of immunosuppressive therapy in patients with virus-negative inflammatory cardiomyopathy: the TIMIC study.', *Eur Heart J* **30**(16), 1995–2002.

Givertz, M. M. & Mann, D. L. (2013), 'Epidemiology and natural history of recovery of left ventricular function in recent onset dilated cardiomyopathies.', *Curr Heart Fail Rep* **10**(4), 321–30.

Gulati, A., Jabbour, A., Ismail, T. F., Guha, K., Khwaja, J., Raza, S., Morarji, K., Brown, T. D., Ismail, N. A., Dweck, M. R., Di Pietro, E., Roughton, M., Wage, R., Daryani, Y., O'Hanlon, R., Sheppard, M. N., Alpendurada, F., Lyon, A. R., Cook, S. A., Cowie, M. R., Assomull, R. G., Pennell, D. J. & Prasad, S. K. (2013), 'Association of fibrosis with mortality and sudden cardiac death in patients with nonischemic dilated cardiomyopathy.', *JAMA* **309**(9), 896–908.

Gutberlet, M., Spors, B., Thoma, T., Bertram, H., Denecke, T., Felix, R., Noutsias, M., Schultheiss, H. P. & Kuhl, U. (2008), 'Suspected chronic myocarditis at cardiac MR: diagnostic accuracy and association with immunohistologically detected inflammation and viral persistence.', *Radiology* **246**(2), 401–9.

Hauck, A. J., Kearney, D. L. & Edwards, W. D. (1989), 'Evaluation of postmortem endomyocardial biopsy specimens from 38 patients with lymphocytic myocarditis: implications for role of sampling error.', *Mayo Clin Proc* **64**(10), 1235–45.

Heiberg, E., Engblom, H., Engvall, J., Hedstrom, E., Ugander, M. & Arheden, H. (2005), 'Semi-automatic quantification of myocardial infarction from delayed contrast enhanced magnetic resonance imaging.', *Scand Cardiovasc J* **39**(5), 267–75.

Hershberger, R. E., Lindenfeld, J., Mestroni, L., Seidman, C. E., Taylor, M. R. G., Towbin, J. A. & , H. F. S. o. A. (2009), 'Genetic evaluation of cardiomyopathy–a Heart Failure Society of America practice guideline.', *J Card Fail* **15**(2), 83–97.

Hiramitsu, S., Morimoto, S., Kato, S., Uemura, A., Kubo, N., Kimura, K., Sugiura, A., Itoh, T. & Hishida, H. (2001), 'Transient ventricular wall thickening in acute myocarditis: a serial echocardiographic and histopathologic study.', *Jpn Circ J* **65**(10), 863–6.

Ismail, T. F., Prasad, S. K. & Pennell, D. J. (2012), 'Prognostic importance of

late gadolinium enhancement cardiovascular magnetic resonance in cardiomyopathy.', *Heart* **98**(6), 438–42.

Karjalainen, J. & Heikkila, J. (1986), '"acute pericarditis": myocardial enzyme release as evidence for myocarditis'.

Kawai, C. (1999), 'From myocarditis to cardiomyopathy: mechanisms of inflammation and cell death: learning from the past for the future.', *Circulation* **99**(8), 1091–100.

Kazanegra, R., Cheng, V., Garcia, A., Krishnaswamy, P., Gardetto, N., Clopton, P. & Maisel, A. (2001), 'A rapid test for B-type natriuretic peptide correlates with falling wedge pressures in patients treated for decompensated heart failure: a pilot study.', *J Card Fail* **7**(1), 21–9.

Kim, R. J., Fieno, D. S., Parrish, T. B., Harris, K., Chen, E. L., Simonetti, O., Bundy, J., Finn, J. P., Klocke, F. J. & Judd, R. M. (1999), 'Relationship of MRI delayed contrast enhancement to irreversible injury, infarct age, and contractile function.', *Circulation* **100**(19), 1992–2002.

Kim, R. J., Wu, E., Rafael, A., Chen, E. L., Parker, M. A., Simonetti, O., Klocke, F. J., Bonow, R. O. & Judd, R. M. (2000), 'The use of contrast-enhanced magnetic resonance imaging to identify reversible myocardial dysfunction.', *N Engl J Med* **343**(20), 1445–53.

Kindermann, I., Barth, C., Mahfoud, F., Ukena, C., Lenski, M., Yilmaz, A., Klingel, K., Kandolf, R., Sechtem, U., Cooper, L. T. & Böhm, M. (2012), 'Update on myocarditis.', *J Am Coll Cardiol* **59**(9), 779–792.

Koitabashi, N. & Kass, D. A. (2012), 'Reverse remodeling in heart failure–mechanisms and therapeutic opportunities.', *Nat Rev Cardiol* **9**(3), 147–157.

Kubanek, M., Malek, I., Bytesnik, J., Fridl, P., Riedlbauchova, L., Karasova, L., Lanska, V. & Kautzner, J. (2006), 'Decrease in plasma B-type natriuretic peptide early after initiation of cardiac resynchronization therapy predicts clinical improvement at 12 months.', *Eur J Heart Fail* **8**(8), 832–40.

Laissy, J. P., Hyafil, F., Feldman, L. J., Juliard, J. M., Schouman-Claeys, E., Steg, P. G. & Faraggi, M. (2005), 'Differentiating acute myocardial infarction from myocarditis: diagnostic value of early- and delayed-perfusion cardiac MR imaging.', *Radiology* **237**(1), 75–82.

Laissy, J. P., Messin, B., Varenne, O., Iung, B., Karila-Cohen, D., Schouman-Claeys, E. & Steg, P. G. (2002), 'MRI of acute myocarditis: a comprehensive approach based on various imaging sequences.', *Chest* **122**(5), 1638–48.

Lang, R. M., Bierig, M., Devereux, R. B., Flachskampf, F. A., Foster, E., Pellikka, P. A., Picard, M. H., Roman, M. J., Seward, J., Shanewise, J. S., Solomon, S. D., Spencer, K. T., Sutton, M. S. & Stewart, W. J. (2005), 'Recommendations for chamber quantification: a report from the American Society of Echocardiography's Guidelines and Standards Committee and the Chamber Quantification Writing Group, developed

in conjunction with the European Association of Echocardiography, a branch of the European Society of Cardiology.', *J Am Soc Echocardiogr* **18**(12), 1440–63.

Lehrke, S., Lossnitzer, D., Schöb, M., Steen, H., Merten, C., Kemmling, H., Pribe, R., Ehlermann, P., Zugck, C., Korosoglou, G., Giannitsis, E. & Katus, H. A. (2011), 'Use of cardiovascular magnetic resonance for risk stratification in chronic heart failure: prognostic value of late gadolinium enhancement in patients with non-ischaemic dilated cardiomyopathy.', *Heart* **97**(9), 727–732.

Leong, D. P., Chakrabarty, A., Shipp, N., Molaee, P., Madsen, P. L., Joerg, L., Sullivan, T., Worthley, S. G., De Pasquale, C. G., Sanders, P. & Selvanayagam, J. B. (2012), 'Effects of myocardial fibrosis and ventricular dyssynchrony on response to therapy in new-presentation idiopathic dilated cardiomyopathy: insights from cardiovascular magnetic resonance and echocardiography.', *Eur Heart J* **33**(5), 640–8.

Levey, A. S., Bosch, J. P., Lewis, J. B., Greene, T., Rogers, N. & Roth, D. (1999), 'A more accurate method to estimate glomerular filtration rate from serum creatinine: a new prediction equation. Modification of Diet in Renal Disease Study Group.', *Ann Intern Med* **130**(6), 461–70.

Lopes, L. R. & Elliott, P. M. (2013), 'Genetics of heart failure.', *Biochim Biophys Acta* **1832**(12), 2451–61.

Loud, A. V. & Anversa, P. (1984), 'Morphometric analysis of biologic processes.', *Lab Invest* **50**(3), 250–61.

Mahrholdt, H., Goedecke, C., Wagner, A., Meinhardt, G., Athanasiadis, A., Vogelsberg, H., Fritz, P., Klingel, K., Kandolf, R. & Sechtem, U. (2004), 'Cardiovascular magnetic resonance assessment of human myocarditis: a comparison to histology and molecular pathology.', *Circulation* **109**(10), 1250–8.

Mahrholdt, H., Wagner, A., Deluigi, C. C., Kispert, E., Hager, S., Meinhardt, G., Vogelsberg, H., Fritz, P., Dippon, J., Bock, C. T., Klingel, K., Kandolf, R. & Sechtem, U. (2006), 'Presentation, patterns of myocardial damage, and clinical course of viral myocarditis.', *Circulation* **114**(15), 1581–90.

Mahrholdt, H., Wagner, A., Judd, R. M., Sechtem, U. & Kim, R. J. (2005), 'Delayed enhancement cardiovascular magnetic resonance assessment of non-ischaemic cardiomyopathies.', *Eur Heart J* **26**(15), 1461–1474.

Maisch, B., Pankuweit, S., Koelsch, S., Hufnagel, G., Funck, R., Grimm, W., Sattler, A. & for the ESETCID Investigators (2007), 'Sequential analysis of immunosuppressive therapy in autoreactive myocarditis - Sequential Analysis from ESETCID.', *Circulation* **116**(16), 337–338.

Maron, B. J., Towbin, J. A., Thiene, G., Antzelevitch, C., Corrado, D., Arnett, D., Moss, A. J., Seidman, C. E. & Young, J. B. (2006), 'Contemporary definitions and classification of the cardiomyopathies: an American Heart Association Scientific Statement from the Council on Clinical Cardiology, Heart Failure and Transplantation Committee; Quality of Care and Outcomes Research and Functional Genomics and Transla-

tional Biology Interdisciplinary Working Groups; and Council on Epidemiology and Prevention.', *Circulation* **113**(14), 1807–16.

Mavrogeni, S., Douskou, M. & Manoussakis, M. N. (2011), 'Contrast-enhanced CMR imaging reveals myocardial involvement in idiopathic inflammatory myopathy without cardiac manifestations.', *JACC Cardiovasc Imaging* **4**(12), 1324–5.

McNamara, D. M., Holubkov, R., Starling, R. C., Dec, G. W., Loh, E., Torre-Amione, G., Gass, A., Janosko, K., Tokarczyk, T., Kessler, P., Mann, D. L. & Feldman, A. M. (2001), 'Controlled trial of intravenous immune globulin in recent-onset dilated cardiomyopathy.', *Circulation* **103**(18), 2254–9.

McNamara, D. M., Starling, R. C., Cooper, L. T., Boehmer, J. P., Mather, P. J., Janosko, K. M., Gorcsan, J., r., Kip, K. E. & Dec, G. W. (2011), 'Clinical and demographic predictors of outcomes in recent onset dilated cardiomyopathy: results of the IMAC (Intervention in Myocarditis and Acute Cardiomyopathy)-2 study.', *J Am Coll Cardiol* **58**(11), 1112–8.

Merlo, M., Pivetta, A., Pinamonti, B., Stolfo, D., Zecchin, M., Barbati, G., Di Lenarda, A. & Sinagra, G. (2014), 'Long-term prognostic impact of therapeutic strategies in patients with idiopathic dilated cardiomyopathy: changing mortality over the last 30 years.', *Eur J Heart Fail* **16**(3), 317–324.

Merlo, M., Pyxaras, S. A., Pinamonti, B., Barbati, G., Di Lenarda, A. & Sinagra, G. (2011), 'Prevalence and prognostic significance of left ventricular reverse remodeling in dilated cardiomyopathy receiving tailored medical treatment.', *J Am Coll Cardiol* **57**(13), 1468–76.

Miller, D. D., Holmvang, G., Gill, J. B., Dragotakes, D., Kantor, H. L., Okada, R. D. & Brady, T. J. (1989), 'MRI detection of myocardial perfusion changes by gadolinium-DTPA infusion during dipyridamole hyperemia.', *Magn Reson Med* **10**(2), 246–55.

Mosterd, A. & Hoes, A. W. (2007), 'Clinical epidemiology of heart failure.', *Heart* **93**(9), 1137–46.

Nishimura, R. A. & Tajik, A. J. (1997), 'Evaluation of diastolic filling of left ventricle in health and disease: Doppler echocardiography is the clinician's Rosetta Stone.', *J Am Coll Cardiol* **30**(1), 8–18.

Ong, P., Athansiadis, A., Hill, S., Kispert, E. M., Borgulya, G., Klingel, K., Kandolf, R., Sechtem, U. & Mahrholdt, H. (2011), 'Usefulness of pericardial effusion as new diagnostic criterion for noninvasive detection of myocarditis.', *Am J Cardiol* **108**(3), 445–52.

Paajanen, H., Brasch, R. C., Schmiedl, U. & Ogan, M. (1987), 'Magnetic resonance imaging of local soft tissue inflammation using gadolinium-DTPA.', *Acta Radiol* **28**(1), 79–83.

Pasotti, M., Klersy, C., Pilotto, A., Marziliano, N., Rapezzi, C., Serio, A., Mannarino, S., Gambarin, F., Favalli, V., Grasso, M., Agozzino, M., Campana, C., Gavazzi,

A., Febo, O., Marini, M., Landolina, M., Mortara, A., Piccolo, G., Vigano, M., Tavazzi, L. & Arbustini, E. (2008), 'Long-term outcome and risk stratification in dilated cardiolaminopathies.', *J Am Coll Cardiol* **52**(15), 1250–60.

Peduzzi, P., Concato, J., Feinstein, A. R. & Holford, T. R. (1995), 'Importance of events per independent variable in proportional hazards regression analysis. Accuracy and precision of regression estimates.', *J Clin Epidemiol* **48**(12), 1503–1510.

Pumannova, M., Roubalova, K., Vitek, A. & Sajdova, J. (2006), 'Comparison of quantitative competitive polymerase chain reaction-enzyme-linked immunosorbent assay with LightCycler-based polymerase chain reaction for measuring cytomegalovirus DNA in patients after hematopoietic stem cell transplantation.', *Diagn Microbiol Infect Dis* **54**(2), 115–20.

Quinones, M. A., Otto, C. M., Stoddard, M., Waggoner, A. & Zoghbi, W. A. (2002), 'Recommendations for quantification of Doppler echocardiography: a report from the Doppler Quantification Task Force of the Nomenclature and Standards Committee of the American Society of Echocardiography.', *J Am Soc Echocardiogr* **15**(2), 167–84.

Richardson, P., McKenna, W., Bristow, M., Maisch, B., Mautner, B., O'Connell, J., Olsen, E., Thiene, G., Goodwin, J., Gyarfas, I., Martin, I. & Nordet, P. (1996), 'Report of the 1995 World Health Organization/International Society and Federation of Cardiology Task Force on the Definition and Classification of cardiomyopathies.', *Circulation* **93**(5), 841–2.

Rieker, O., Mohrs, O., Oberholzer, K., Kreitner, K. F. & Thelen, M. (2002), 'Cardiac MRI in suspected myocarditis.', *Rofo* **174**(12), 1530–6.

Schrier, R. W. & Abraham, W. T. (1999), 'Hormones and hemodynamics in heart failure.', *N Engl J Med* **341**(8), 577–85.

Shanes, J. G., Ghali, J., Billingham, M. E., Ferrans, V. J., Fenoglio, J. J., Edwards, W. D., Tsai, C. C., Saffitz, J. E., Isner, J., Furner, S. & et al. (1987), 'Interobserver variability in the pathologic interpretation of endomyocardial biopsy results.', *Circulation* **75**(2), 401–5.

Sherwood, M. W. & Kristin Newby, L. (2014), 'High-sensitivity troponin assays: evidence, indications, and reasonable use.', *J Am Heart Assoc* **3**(1), e000403.

Shirani, J., Freant, L. J. & Roberts, W. C. (1993), 'Gross and semiquantitative histologic findings in mononuclear cell myocarditis causing sudden death, and implications for endomyocardial biopsy.', *Am J Cardiol* **72**(12), 952–7.

Steimle, A. E., Stevenson, L. W., Fonarow, G. C., Hamilton, M. A. & Moriguchi, J. D. (1994), 'Prediction of improvement in recent onset cardiomyopathy after referral for heart transplantation.', *J Am Coll Cardiol* **23**(3), 553–9.

Virtova, R., Kubanek, M., Sramko, M., Voska, L., Kautznerova, D. & Kautzner, J. (2013), 'Isolated non-compaction cardiomyopathy: A review.', *Cor et Vasa* (55), 236–241.

Voigt, A., Elgeti, T., Durmus, T., Idiz, M. E., Butler, C., Beling, M., Schilling, R., Klingel, K., Kandolf, R., Stangl, K., Taupitz, M., Kivelitz, D. & Wagner, M. (2011), 'Cardiac magnetic resonance imaging in dilated cardiomyopathy in adults–towards identification of myocardial inflammation.', *Eur Radiol* **21**(5), 925–35.

Wilcox, J. E., Fonarow, G. C., Yancy, C. W., Albert, N. M., Curtis, A. B., Heywood, J. T., Inge, P. J., McBride, M. L., Mehra, M. R., O'Connor, C. M., Reynolds, D., Walsh, M. N. & Gheorghiade, M. (2012), 'Factors associated with improvement in ejection fraction in clinical practice among patients with heart failure: findings from IMPROVE HF.', *Am Heart J* **163**(1), 49–56 e2.

WMA (2004), 'World Medical Association Declaration of Helsinki: ethical principles for medical research involving human subjects.', *J Int Bioethique* **15**(1), 124–9.

Wu, K. C., Weiss, R. G., Thiemann, D. R., Kitagawa, K., Schmidt, A., Dalal, D., Lai, S., Bluemke, D. A., Gerstenblith, G., Marbán, E., Tomaselli, G. F. & Lima, J. A. C. (2008), 'Late gadolinium enhancement by cardiovascular magnetic resonance heralds an adverse prognosis in nonischemic cardiomyopathy.', *J Am Coll Cardiol* **51**(25), 2414–2421.

Yilmaz, A., Mahrholdt, H., Athanasiadis, A., Vogelsberg, H., Meinhardt, G., Voehringer, M., Kispert, E. M., Deluigi, C., Baccouche, H., Spodarev, E., Klingel, K., Kandolf, R. & Sechtem, U. (2008), 'Coronary vasospasm as the underlying cause for chest pain in patients with PVB19 myocarditis.'.

Zagrosek, A., Wassmuth, R., Abdel-Aty, H., Rudolph, A., Dietz, R., Schulz-Menger, J., Yilmaz, A., Mahrholdt, H., Athanasiadis, A., Vogelsberg, H., Meinhardt, G., Voehringer, M., Kispert, E. M., Deluigi, C., Baccouche, H., Spodarev, E., Klingel, K., Kandolf, R. & Sechtem, U. (2009), 'Cardiac magnetic resonance monitors reversible and irreversible myocardial injury in myocarditis.', *J Cardiovasc Magn Reson* **2**(2), 141–8.

Appendix – own publications related to the topic

Paper 1 — "Utility of combination of cardiac magnetic resonance imaging and high-sensitivity cardiac troponin T assay in diagnosis of inflammatory cardiomyopathy."
Sramko M, Kubanek M, Tintera J, Kautznerova D, Weichet J, Maluskova J, Franeková J, Kautzner J.
Am J Cardiol. 2013;111(2):258-64. (IF 3.5)

Paper 2 — "Novel predictors of left ventricular reverse remodeling in individuals with recent-onset dilated cardiomyopathy."
Kubanek M, **Sramko M**, Maluskova J, Kautznerova D, Weichet J, Lupinek P, Vrbska J, Malek I, Kautzner J.
J Am Coll Cardiol. 2013;61(1):54-63. (IF 15.3)